Energy and Electron Transfer in a Poly(fluorene-*alt*-phenylene) Bearing Perylenediimides as Pendant Electron Acceptor Groups

Rafael Gómez,[†,‡] Dirk Veldman,[‡] Raúl Blanco,[†] Carlos Seoane,[†] José L. Segura,*[,†] and René A. J. Janssen*[,‡]

Departamento de Química Orgánica, Facultad de Química, Universidad Complutense de Madrid, E-28040, Madrid, Spain, and Macromolecular and Organic Chemistry, Eindhoven University of Technology, P.O. Box 513, 5600 MB Eindhoven, The Netherlands

Received January 4, 2007; Revised Manuscript Received February 7, 2007

ABSTRACT: We describe the synthesis and characterization of a novel poly(fluorene-*alt*-phenylene) substituted with perylenediimide (PDI) moieties as pendant groups. Cyclic voltammetry experiments show the amphoteric nature of the material, which combines the good electron donor ability of the polymeric chain with the acceptor properties of the pendant PDI moieties. Absorption spectroscopy suggests the presence of PDI aggregates, whereas the emission spectra show a strong emission quenching of both the polymeric backbone and the PDI units. Further investigation on the energy and/or electron-transfer processes involved is carried out by temperature-dependent excitation spectra and photoluminescence lifetimes. These studies show the presence of electron transfer not only from the electron donor polymeric chain to the pendant PDI units but also, and more remarkably, to PDI aggregates both in solution and in solid state, as is further confirmed by photoinduced absorption spectroscopy.

Introduction

The use of photoactive organic compounds as materials for organic light-emitting diodes (OLEDs)[1] and plastic solar cells[2] has gained significant attention in the past decade. Both photoactive polymers[3] and small-size functional molecules[4,5] have been successfully employed in the fabrication of this kind of optoelectronic devices. Among conjugated polymers, polyfluorene (PF) derivatives have played a key role in the development of optoelectronic devices due to their high photoluminescence (PL) and electroluminescence (EL) efficiencies and good thermal stabilities. Furthermore, facile methods for functionalizing the C9 position of the fluorene unit offer the possibility of tuning the optoelectronic properties of PF and to obtain materials with enhanced solubility and film forming ability.[6,7]

On the other hand, perylenediimide (PDI)-based colorants have received a great deal of attention not only in academic but also as industrial dye and in pigment research.[8] More recently, PDI derivatives have developed into one of the best n-type semiconductors available to date[9] and have found application in different areas such as organic solar cells[5,10] or field effect transistors,[11] among others.[12−15] In parallel with the different applications found for PDI derivatives, a broad range of derivatives have been synthesized, including derivatives with extended π-conjugation,[16] multi-PDI systems,[17] supramolecular architectures,[18,19] and a number of PDI derivatives covalently linked to electroactive moieties.[20−28]

One of the most active areas of research involving PDI systems is related to their implications in photoinduced energy and/or electron-transfer processes. In this regard, Müllen and co-workers have incorporated perylenemonoimide and PDI dyes into shape-persistent dendrimers, allowing the investigation of dye−dye interactions at the single molecule level.[29]

* To whom correspondence should be addressed: (R.J.) phone +31 40 2473597, e-mail r.a.j.janssen@tue.nl; (J.L.S.) phone +34-91-3945142, e-mail segura@quim.ucm.es.

[†] Universidad Complutense de Madrid.

[‡] Eindhoven University of Technology.

Conjugated oligomers such as oligothiophenes,[30] oligo(*p*-phenylenevinylene)s,[31−34] oligo(*p*-phenylene)s,[35] and oligopyrroles[36] have also been covalently linked to perylenemonoimide and PDI dyes, and their photophysical properties have been investigated.

Besides, there has been increasing interest in the morphology of organic semiconductors in films because of its strong influence on device performance. In this regard, PDI derivatives have been covalently linked as side chains to poly(methyl methacrylate)[37] and poly(isocyanide)[38] and have been incorporated in the main chain of copolymers[39] and supramolecular polymers.[40]

Some efforts have also been dedicated to the synthesis of systems that contain oligo- and polyfluorenes covalently linked to perylenemonoimide and PDI derivatives (Figure 1). Wasielewski and co-workers have investigated oligofluorenes as molecular wires (**1**, Figure 1).[41] Electron transfer was identified after excitation of derivatives **1**, but not in the reference systems **2** containing only oligofluorenes and PDI.

Others have attached peryleneimides at the end of oligofluorene chains. The resulting materials (**3**, Figure 1) do not show energy transfer in solution, but an almost complete transfer of excitation energy to the perylenemonoimides is observed in the solid state.[42] Copolymers **4** (Figure 1) have also been synthesized using 1% and 5% of PDI comonomer,[42a] and as it might be expected for materials containing only low amounts of the dye chromophores, in solution they show the absence of energy transfer. However, in the solid state, efficient energy transfer to the chromophores occurs. Similarly, no energy transfer is observed in solution for polymers **5**.[43]

A different type of perylene containing polymer (**6**, Figure 1) has been synthesized, for which the design permits the incorporation of a higher concentration of perylene dye without affecting the electronic properties of the polyfluorene backbone.[42a] Whereas the previous types of polymers, in which the perylene units are directly attached to the main chain, show energy transfer only in the solid state, efficient energy transfer to the

10.1021/ma070026b CCC: $37.00
Published on Web 03/17/2007

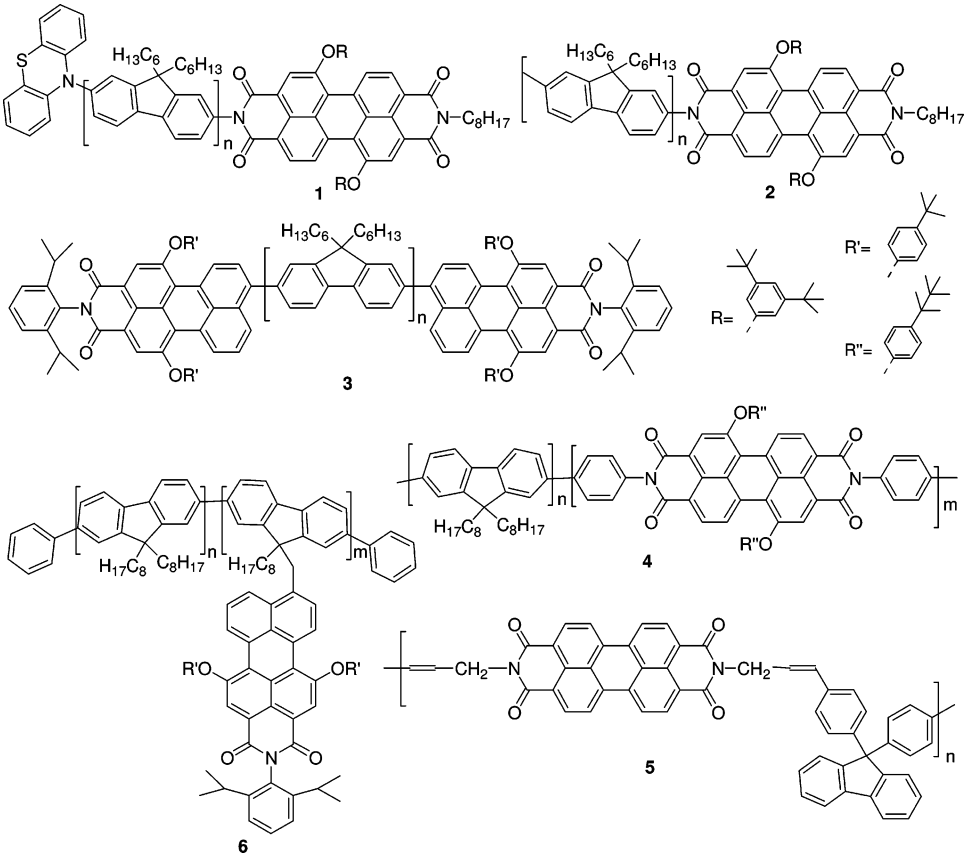

Figure 1. Selected peryleneimide-containing oligo- and polyfluorenes.

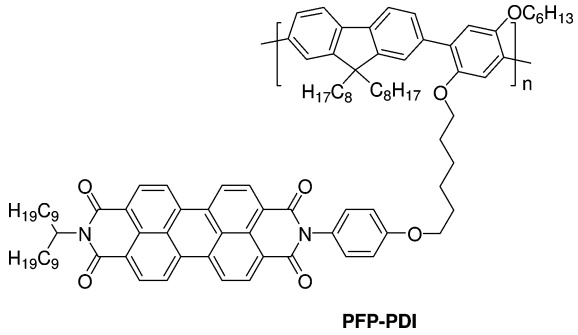

Figure 2. Donor−acceptor polymer PFP−PDI.

pendant groups is clearly observed in the photoluminescence (PL) spectrum of **6**.

In this article we describe the synthesis of a new poly(fluorene-*alt*-phenylene) (PFP) derivative bearing PDI moieties attached as pendant groups (PFP−PDI, Figure 2). The presence of the electron-rich dialkoxybenzene units in polymer PFP−PDI increases the electron-donating ability of the polymeric chain, in comparison with that of the parent polyfluorene (PF) system, which, as shown above, by itself is not a strong enough donor against PDI to result in electron transfer. This fact is, therefore, of great importance to investigate this polymeric chain in combination with electron acceptor systems.

The strong tendency of PDI derivatives to π-stack and construct one-dimensional aggregates has been well established in the solid state[44] and in solution.[45] In this regard, Wasielewski and co-workers have also investigated extensively the self-assembly of PDI derivatives driven primarily by strong van der Waals interactions between the PDI molecules.[17f,46] For some of these derivatives, PDI molecules stack to form aggregates in which energy transfer processes take place not from individual molecules but from the aggregated PDI molecules.[47]

Whereas the presence of low concentrations of PDI units in compounds **1**−**5** prevents the observation of aggregation phenomena and, thus, excitation energy transfer occurs without the participation of PDI aggregates, the synthetic strategy used for the synthesis of PFP−PDI incorporates a high concentration of PDI units as side groups and enables the aggregation of PDI moieties in the polymer. Moreover, the polymeric architecture enhances the $\pi-\pi$ stacking interaction between the perylene units.

Thus, in this article we describe the synthesis and the photophysical processes of the first fluorene-based copolymer containing covalently linked PDI units that exhibits photoinduced electron transfer not only to the individual PDI moieties but also to aggregated PDI units.

Results and Discussion

Synthesis. The preparation of the donor−acceptor poly(fluorene-*alt*-phenylene) bearing PDI units (PFP−PDI) and the reference poly(fluorene-*alt*-phenylene) (PFP) was carried out using the classical palladium-catalyzed Suzuki[48] coupling reaction between the appropriately functionalized monomers. This approach has the advantage to yield structurally well-defined alternating copolymers.

Synthesis of Monomers. The synthesis of the suitably functionalized monomer **12** bearing PDI units is shown in Scheme 1. In order to enhance the solubility and processability, we have chosen a long nonconjugated alkyl spacer between the PFP backbone and the PDI groups, which is also expected to improve the conformational flexibility of the side groups with respect to the chain.

Thus, the Williamson etherification reaction between 4-hexyloxy-2,5-diiodophenol (**7**)[49] and 1-bromo-6-chlorohexane (**8**) using potassium carbonate as the base and a catalytic amount

Scheme 1. Synthesis of PDI Monomer 12

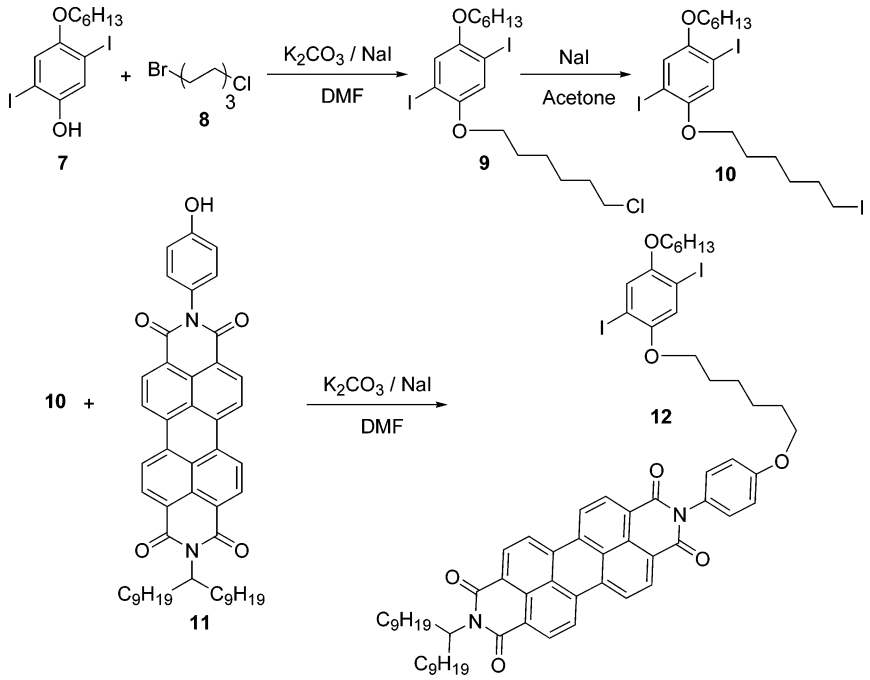

Scheme 2. Synthesis of Polymer PFP−PDI

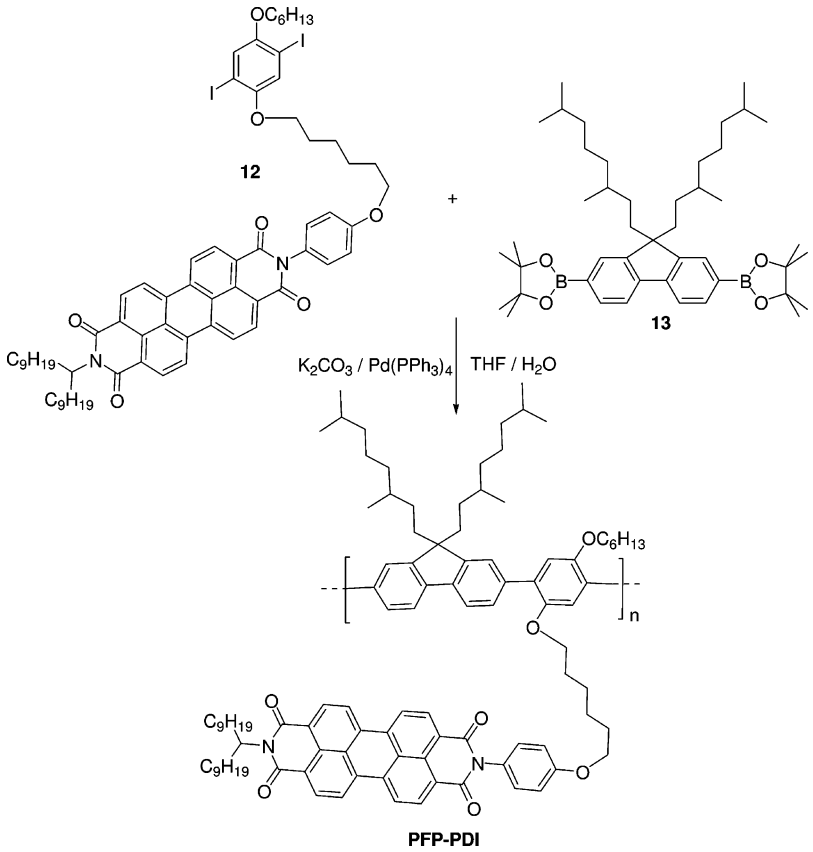

of potassium iodide afforded derivative **9**. The low tendency of the chlorine atom in **8** to act as a leaving group allows the regioselective etherification between **7** and **8**. The less reactive chlorine atom in **9** is then interchanged in a Finkelstein reaction by iodine, having a better leaving group character. A further Williamson etherification reaction between **10** and the complementarily functionalized *N*-(4-hydoxyphenyl)-*N*′-(10-nonadecyl)perylene-3,4:9,10-bis(dicarboximide) (**11**)[50] using potassium carbonate as the base in refluxing DMF afforded monomer **12** in a moderate 37% yield. The introduction of long swallow-tail solubilizing chains in the PDI unit together with the two hexyloxy groups on the benzene ring provides monomer **12** enough solubility to be further polymerized.

Synthesis of Donor−Acceptor Polymer PFP−PDI. The target polymer PFP−PDI was synthesized by a Suzuki polycondensation of an equimolecular mixture of the diiodo-functionalized monomer **12** and the 2,7-bis(4,4,5,5-tetramethyl-1,3,2-dioxaborolan-2-yl)-9,9-(3,7-dimethyloctyl)fluorene (**13**)[51]

Scheme 3. Synthesis of Reference Polymer PFP and Chemical Structure of Reference Dialkyl-PDI

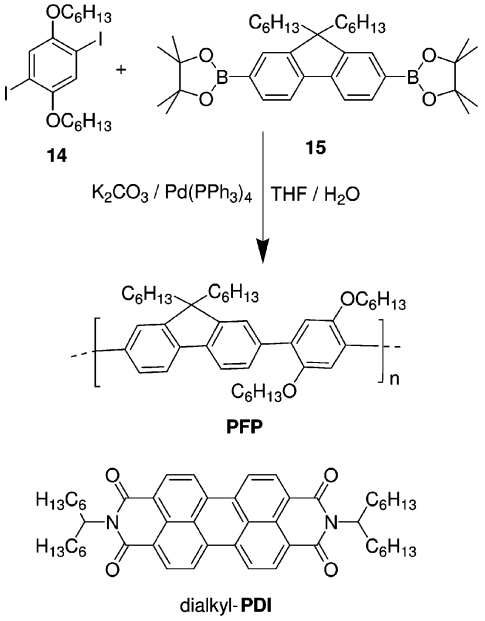

in the presence of 5 mol % $Pd(PPh_3)_4$ in a mixture of dry degassed THF and aqueous potassium carbonate for 48 h under reflux (Scheme 2). Although boronic acids have been often directly used as reagents in poly-Suzuki couplings, boronic esters like **13** have proven to be more advantageous in this kind of reaction, since the presence of the 1,1,2,2-tetramethylethylene glycol units has a protective effect on the labile boronic acid precursor. Simultaneously to the polymerization, a hydroxylation deprotection process takes place, in which the removal of such protecting groups as ethylene glycol does not affect the couplings.[52] The resulting well-defined alternating copolymer PFP−PDI was then precipitated out of the thick reaction mixture by addition of methanol, purified by reprecipitation from chloroform/methanol and thoroughly washed with additional methanol and diethyl ether to remove ionic species and unreacted materials. Thus, the PFP−PDI polymer, in which a poly(fluorene-*alt*-phenylene) polymeric chain is endowed with PDI units as pendant groups, could be obtained in nearly quantitative yield as a bright red solid.

In order to be used as a reference material in the photophysical investigations, we have also synthesized copolymer PFP by an analogous Suzuki polycondensation between 1,4-dihexyloxy-2,5-diiodobenzene (**14**)[53] and bisborolane **15**[54] under the same conditions as previously described for PFP−PDI (Scheme 3). Following the same experimental procedure, PFP was precipitated out of the reaction mixture and further reprecipitated from methanol, to give PFP as a beige solid in 87% yield.

The good solubility of PFP−PDI and PFP polymers in common organic solvents enabled their characterization by size exclusion chromatography (SEC), NMR, optical and electrochemical techniques, and further photophysical investigations. Of the two compounds, PFP−PDI shows an increased solubility, presumably due to the presence of the additional swallow tails on the PDI units.

Taking into account their structural resemblance, the ^{1}H NMR spectra of PFP−PDI and PFP display the signals corresponding to the alkyl chains at high fields and those of the alkoxy groups at around 4 ppm as common features. In contrast to monomer **12**, in which the nonequivalent alkoxy protons appear as three overlapping triplets, in PFP−PDI and PFP a broad singlet is observed for those protons, as is often observed in other polymeric materials. The remaining signals corresponding to the benzene and fluorene backbone are also displayed at low fields (7.0−7.8 ppm) with certain similarity. In the case of PFP−PDI, the presence of the PDI units gives rise to additional signals with respect to reference polymer PFP. Thus, the distinctive expected signals at low fields (8.7−8.2 ppm) for the aromatic PDI protons are clearly visible. The ^{1}H NMR spectrum of PFP−PDI is completed by the signal at 5.2 ppm for the proton directly linked to the imide nitrogen as a broad singlet. The FTIR spectrum of PFP−PDI further proves its structure and contains the typical strong bands at 1699 and 1653 cm^{-1} for imide groups and also the characteristic absorption pattern of the perylene skeleton with bands around 1580 and 1590 cm^{-1}.[55] Finally, evidence concerning the purity of PFP, PFP−PDI, and all the intermediates used in their synthesis is given by elemental analysis, which is in accordance with the expected values.

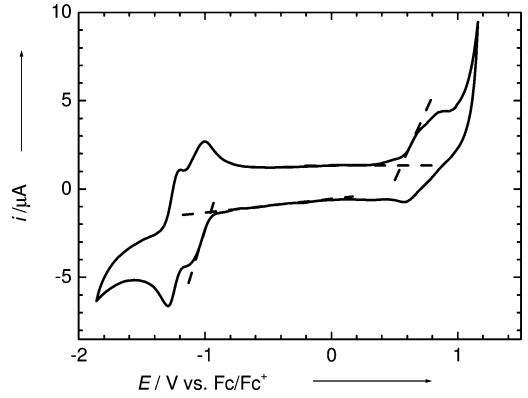

Figure 3. Cyclic voltammogram of PFP−PDI copolymer in dichloromethane solution. Pt was used as working and counter electrode and $TBAPF_6$ as supporting electrolyte, at a scan rate of 200 mV s^{-1}.

The molecular weights of PFP−PDI and PFP were determined by SEC analysis in *o*-dichlorobenzene (*o*-DCB) at 80 °C using polystyrene standards and show M_w and M_n values of 101 000 and 16 400 g/mol (pd = 6.2) for PFP−PDI and 38 000 and 13 100 g/mol (pd = 2.9) for reference compound PFP. A bimodal behavior is observed in the time trace of PFP−PDI, with peak molecular weights of M_p = 20 170 and 82 500 g/mol. Probably this is due to aggregation phenomena at the concentration used in the SEC experiment (1−0.5 mg mL^{-1}).

Electrochemistry. The redox properties of the novel electroactive donor−acceptor copolymer PFP−PDI were determined by cyclic voltammetry measurements at room temperature in dichloromethane solution, using a platinum disk and wire as working and counter electrodes, respectively, Ag/AgCl as reference electrode, and tetrabutylammonium hexafluorophosphate ($TBAPF_6$, 0.1 M) as supporting electrolyte. The ferrocene/ferrocenium (Fc/Fc^+) couple was used as internal reference and showed a peak at +0.35 eV vs Ag/AgCl.

The cyclic voltammogram of PFP−PDI (Figure 3) shows the amphoteric behavior of the material. At negative values, two distinct one-electron reversible (−1.05 and −1.25 eV vs Fc/Fc^+) reduction waves corresponding to the PDI moiety are clearly visible. For comparison, the reference compound *N*,*N*′-(1-hexylheptyl)perylene-3,4:9,10-bis(dicarboximide),[56] dialkyl-PDI (Scheme 3), gives peaks at −1.11 and −1.31 eV vs Fc/Fc^+, which is similar to the values reported earlier for PDI compounds.[57,58] It is worth mentioning that the presence of the electron-rich benzylic rings in the PDI unit causes a small change (0.06 eV)[57] on the electronic properties of the PDI because of the presence of nodes of the HOMO and LUMO orbitals at the imide nitrogen.[19a] Thus, the PDI units can be

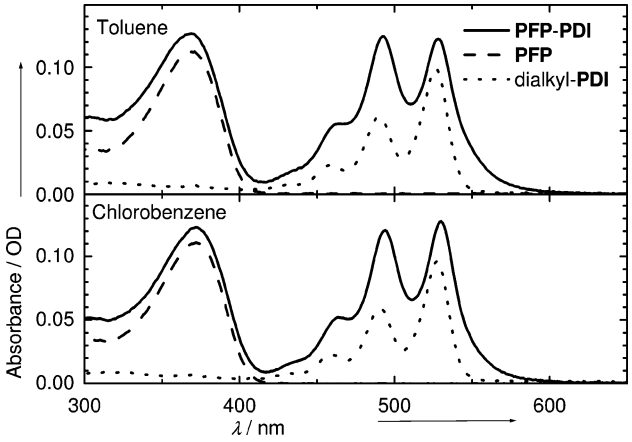

Figure 4. Absorption spectra of PFP−PDI along with references PFP and dialkyl-PDI.

regarded as independent chromophoric systems whose electronic properties remain unaltered by the imide substituent.[59] At positive potentials a broad quasi-irreversible oxidation wave can be detected, with an onset at +0.56 eV vs Fc/Fc^+, which was also found for the reference polymer PFP (+0.55 eV vs Fc/Fc^+) and can, therefore, be assigned to the oxidation of the polymer chain.

The similar values observed for the oxidation and reduction processes of the two electroactive moieties in PFP−PDI compared to the reference compounds suggest that there is no significant ground state interaction between the electron-donating polymer backbone and the electron-accepting PDI moieties.

UV−Vis Absorption Spectra. The UV−vis absorption spectra of the donor−acceptor copolymer PFP−PDI together with that of references PFP and dialkyl-PDI in diluted (ca. 5×10^{-6} M) toluene and chlorobenzene solutions are depicted in Figure 4. The absorption spectrum of PFP−PDI consists of the approximate superposition of the absorption features of its constitutive units, confirming the minimal interaction between the chromophores in the ground state, in agreement with the electrochemical behavior. The spectrum displays an intense absorption band at around 370 nm corresponding to the $\pi-\pi^*$ transition in the fluorene−benzene polymeric backbone as inferred from comparison with the reference compound PFP. Additionally, the absorption spectrum of PFP−PDI shows characteristic bands arising from the presence of the PDI side groups, with maxima in toluene at 528, 492, and 462 nm. However, the comparison of the absorption spectrum of PFP−PDI with that of the dialkyl-PDI reference shows some differences. Thus, the dialkyl-PDI reference shows a maximum of the (0,0) vibronic transition at 527 and a maximum of the (0,1) vibronic at 490 nm, which is 1.62 times lower in intensity (in both toluene and chlorobenzene). This corresponds well to the values found for free perylene units (0,0)/(0,1) ≈ 1.6.[60] In these diluted solutions, dialkyl-PDI can be regarded as completely dissolved (i.e., nonaggregated), as the measured solubility of this compound exceeds 100 g L^{-1} in common organic solvents.[56] Further evidence is given by the absence of any sign of aggregate emission upon photoexcitation. For PFP−PDI, however, the absorption spectrum is bathochromically shifted compared to the dialkyl-PDI. The (0,1) vibronic band shows an increase relative to the (0,0) transition. This is typical for stacking of PDI chromophores in H-aggregates, where the chromophores are cofacially arranged. Strong vibronic coupling in the H-aggregates results in an enhanced (0,1) vibronic band compared to nonaggregated PDI molecules.[17c,e,f,46a] Thus, upon

Table 1. Peak-to-Peak Ratios for the First and the Second Absorption and Fluorescence Peaks of PFP−PDI in the Three Investigated Solvents Compared to the Reference Dialkyl-PDI

	ratio abs[a]	ratio PL[b]
toluene	0.98	8.0
chlorobenzene	1.06	6.0
dichloromethane	1.11	3.5
dialkyl-PDI (toluene, *o*-DCB)	1.62	0.1

[a] Peak-to-peak ratio of the absorbance at 530 and 495 nm, (0,0)/(0,1). [b] Peak-to-peak ratio of the fluorescence at 630 and 535 nm, aggregate/(0,0).

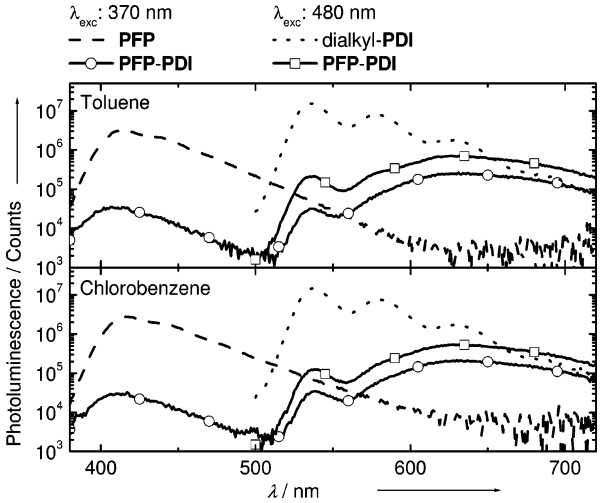

Figure 5. Photoluminescence spectra of PFP, dialkyl-PDI, and PFP−PDI in toluene (top) and chlorobenzene (bottom). Note that the vertical axis gives the logarithm of the PL intensity.

aggregation of PDI, the ratio of the intensities of the (0,0) and the (0,1) transitions decreases, which is often used as an indication of aggregation[47,61] with π-type stacking behavior that can be rationalized by the molecular exciton model.[17c,e,f] Therefore, the observed change in absorption of the PDI units in PFP−PDI with respect to dialkyl-PDI indicates that the PDI units in the polymer are π-stacked. In toluene the intensity of the (0,1) transition is higher than that of the (0,0) one, with a ratio (0,0)/(0,1) of 0.98, indicating more aggregation than in chlorobenzene. For dichloromethane, the observed aggregation seems less than in chlorobenzene (Table 1).

We assume that aggregation takes place predominantly within the polymer chain itself and that intermolecular aggregates do not form at the concentrations of PDI chromophores that we have investigated (ca. 5×10^{-6} M), as it is known that PDI chromophores bearing long alkyl tails do not tend to aggregate up to 10^{-3} M in the solvents investigated.[56] Therefore, in PFP−PDI, the intramolecular aggregation must be induced by the short distance between two consecutive PDI moieties and, hence, the high local concentrations.

Photoluminescence Spectra. The photoluminescence properties of the PFP−PDI donor−acceptor polymer were measured in three solvents with different relative permittivity, i.e., toluene ($\epsilon = 2.43$), chlorobenzene ($\epsilon = 5.47$), and dichloromethane ($\epsilon = 9.02$), which is an indication of the polarity of the solvent. The photoluminescence spectra of PFP−PDI and the two reference materials (PFP and dialkyl-PDI) were recorded (Figure 5) with selective excitation of the PFP backbone ($\lambda_{exc} = 370$ nm) or the PDI side groups ($\lambda_{exc} = 480$ nm).

The singlet excited-state energies of PFP, dialkyl-PDI, and PFP−PDI were determined from the photoluminescence maxima in toluene (Table 2). The energy of the lowest singlet excited state ($S_{1,D}$) of the PFP backbone in polymer PFP−PDI is 0.73

Table 2. Oxidation and Reduction Onset Potentials and Energies of the Lowest Singlet Excited States of PFP−PDI and the Reference Compounds PFP and Dialkyl-PDI

	PFP−PDI	PFP	dialkyl-PDI
$E_{ox,o}$ (eV)	0.56[a]	0.55[b]	
$E_{red,o}$ (eV)	−0.98[a]		−1.03[a]
$S_{1,D}$ (eV)[c]	3.05	3.00	
$S_{1,A}$ (eV)[c]	2.32		2.31

[a] Onset in dichloromethane vs Fc/Fc^+. [b] Onset in *o*-DCB:acetonitrile (4:1) vs Fc/Fc^+. [c] Photoluminescence maxima in toluene.

eV higher than the S_1 of the PDI dangling groups ($S_{1,A}$). Thus, after excitation of the polymer backbone, energy transfer from the PFP to the PDI moieties can be anticipated.

The emission spectra show the same features in the three solvents. The PFP reference polymer shows a broad emission with a maximum at around 415 nm. The dialkyl-PDI reference compound shows the characteristic fluorescence spectrum of nonaggregated PDI with maxima at 536, 579, and 628 nm. Upon excitation of the PFP backbone ($\lambda_{exc} = 370$ nm) the emission spectrum of PFP−PDI shows maxima at 415 nm from the PFP backbone and at 535 nm from the nonaggregated PDI and a broad band around 630 nm. The maximum at 535 nm indicates that energy transfer takes place from the PFP chain to the PDI moieties when the PFP is photoexcited, as the PDI part hardly absorbs at 370 nm. Selective excitation of the PDI units of PFP−PDI ($\lambda_{exc} = 480$ nm) leads to nonaggregated PDI emission (at 535 nm) and again a broad emission with a maximum at 630 nm. This broad emission at 630 nm is characteristic for PDI-based H-aggregates reported so far.[17b,60b,61c,62] The ratio between the emission at 630 nm (coming from $(PDI)_n$) and the emission at 535 nm (from nonaggregated PDI) is an indication of the degree of stacking. In Table 1 it is shown how this ratio decreases in the order toluene > chlorobenzene > dichloromethane. In this way, photoluminescence measurements provide further evidence that the aggregation of the PDI moieties in PFP−PDI is the least in dichloromethane and the most in toluene, as was also the trend observed in the absorption spectra.

The fluorescence quantum yields of the PFP−PDI polymer were measured in the three different solvents (toluene, chlorobenzene, and dichloromethane) relative to PFP ($\lambda_{exc} = 370$ nm, $\lambda_{em} = 415$ nm) and dialkyl-PDI ($\lambda_{exc} = 480$ nm, $\lambda_{em} = 535$ nm), showing a decrease of almost 2 orders of magnitude in all the investigated solvents (Table 3). The strong quenching of the PFP emission in PFP−PDI can be explained in terms of energy transfer from the PFP backbone to the PDI moieties or by electron transfer from the PFP backbone to the PDI accepting units. Similarly, the strong quenching of the PDI emission compared to the reference compound can be explained in two ways: as a result of intramolecular aggregation or as a consequence of electron transfer considering that PDI is a good electron acceptor (vide supra). It should be noted that the extremely small residual emission of nonaggregated PDI units at 530 nm can also be due to an ~1% impurity of another PDI derivative in the polymer. This would imply that the actual quenching from bound PDI units is even more effective.

Steady-State Excitation Spectra. The study of excitation spectra can give evidence about the energy transfer processes taking place in PFP−PDI. The excitation spectra of PFP−PDI in toluene and chlorobenzene were measured at 530 nm (wavelength at which only nonaggregated PDI emits) and 630 nm (at which aggregated PDI emits). The excitation spectra are shown in Figure 6 in comparison to the absorbance spectra of the same solutions. A clear difference between the spectra at 530 and 630 nm can be observed. For the emission at 530 nm the PDI spectral features (>400 nm) are identical to those of a nonaggregated PDI absorbance spectrum, with a ratio of (0,0)/(0,1) = 1.6, similar to dialkyl-PDI in Figure 4. When the emission at 630 nm is probed, it matches the absorbance spectrum of an H-aggregated PDI stack, with a ratio of (0,0)/(0,1) = 0.80. The comparison of the excitation spectra with the absorbance spectrum clarifies that the absorption spectrum contains for the largest part aggregated species with a small contribution of nonaggregated PDI molecules: in the absorbance spectrum there is a higher contribution at 530 nm and a lower contribution at 465 nm compared to the excitation spectrum at 630 nm.

Besides the absorption of PDI, an absorption band of PFP (with maxima around 370 nm) is also present in the excitation spectra. This feature suggests that, upon photoexcitation, energy transfer takes place in the PFP−PDI: once the PFP backbone is excited, it transfers its energy to the PDI moiety. We note that if the 530 nm emission was only due to unbound PDI impurities, the excitation spectrum would not show that feature at 370 nm.

Additionally, from the excitation spectra we infer that energy transfer to aggregated PDI cannot be the only process that leads to quenching of the nonaggregated PDI emission because the excitation spectrum at 630 nm is not the same as the absorbance spectrum: the peak at 530 nm is 15% (in toluene) and 18% (in chlorobenzene) lower in the excitation spectrum than in the absorbance spectrum of PFP−PDI. This means that a part of the nonaggregated PDI that is excited decays via another process than energy transfer to PDI aggregates. Thus, although part of the excited nonaggregated PDI decays via luminescence (with a maximum at 530 nm), the fact that the PL at 530 nm is very weak (only 1% compared to the dialkyl-PDI, Table 3) suggests that a substantial part of the excited PDI decays via electron transfer by accepting an electron from the PFP backbone.

The efficiency of the energy transfer cannot be quantified by correlating the UV/vis absorption with fluorescence excitation spectra because energy transfer from PFP to PDI moieties is not the only process that quenches the PFP emission. In addition, the PDI fluorescence itself will be quenched by aggregation and possibly electron transfer.

Photoluminescence Lifetimes. By investigating the photoluminescence lifetimes at different wavelengths, we can determine whether the lifetime is reduced (i.e., if energy or electron transfer takes place from that nonaggregated state) or increased (i.e., if aggregated species are present). Time-resolved photoluminescence was measured in the same solvents as the steady-state photoluminescence (toluene, chlorobenzene, and dichloromethane) using an excitation wavelength of 400 nm. At this wavelength the PFP backbone is excited primarily. The results of these measurements are shown in Figure 7.

The photoluminescence lifetime of PFP at 415 nm is 0.49 ns in all the three solvents. In PFP−PDI the lifetime of the polymer emission is effectively quenched to shorter (<20 ps) than we could measure with our setup (fwhm = 155 ps for the laser) in the investigated solvents (Figure 7a). This corresponds well to the observations described before, that energy transfer occurs from the PFP to the PDI moieties. The photoluminescence of dialkyl-PDI can be fitted with a monoexponential decay with a lifetime of 4.01 ns in toluene and 3.83 ns in chlorobenzene (Figure 7a), which corresponds well to the value of 3.95 ns earlier reported for this compound in $CHCl_3$.[17a] When probing the PFP−PDI emission at 540 nm, two emission lifetimes can be fitted: a small component (1.5% in toluene, 0.5% in chlorobenzene, and 1.7% in dichloromethane) with a

Table 3. Fluorescence Quantum Yields of the Donor and Acceptor Moiety in Toluene, Chlorobenzene, and Dichloromethane and Results of Eq 1

	ϵ_s	Φ_F (PFP)[a]	Φ_F (PDI)[b]	ΔG_{CS} [eV][c]	E_{CS} [eV][d]
toluene	2.43	0.010	0.014	−0.16	2.16
chlorobenzene	5.47	0.011	0.0083	−0.71	1.61
dichloromethane	9.02	(<0.019)	0.017	−0.85	1.47

[a] Fluorescence quantum yield of PFP−PDI relative to PFP at 415 nm after excitation at 370 nm. [b] Fluorescence quantum yield of PFP−PDI relative to dialkyl-PDI at 535 nm after excitation at 480 nm. [c] Based on eq 1 with $r^+ = 5.0$ Å, $r^- = 4.7$ Å, $R_{cc} = 20$ Å, and $E(S_1) = 2.32$ eV.[63] [d] Using $E_{CS} = E(S_1) - \Delta G_{CS}$.

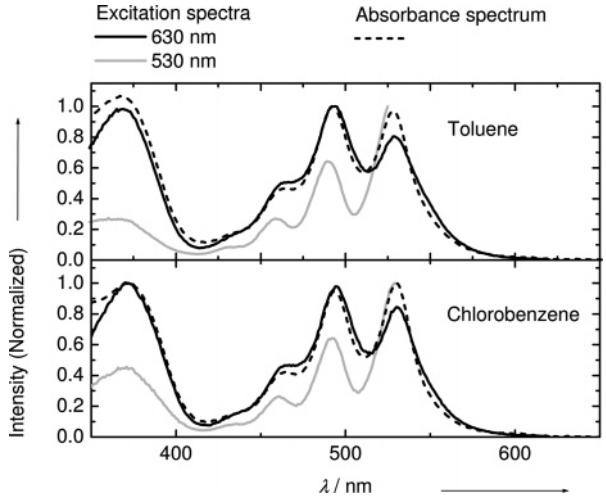

Figure 6. Excitation (solid line) and absorbance (dashed line) spectra of PFP−PDI in toluene (top) and chlorobenzene (bottom).

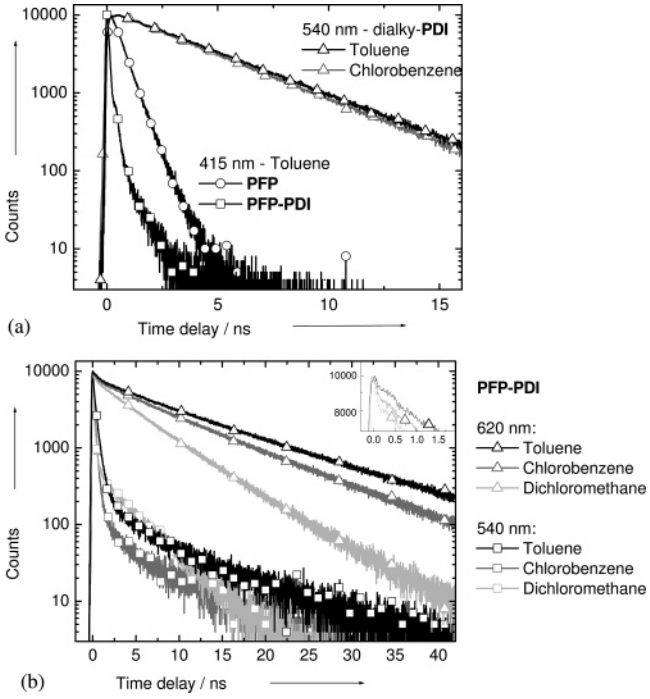

Figure 7. (a, b) Time-resolved photoluminescence data of PFP, dialkyl-PDI, and PFP−PDI at 415, 540, and 620 nm in various solvents upon excitation at 400 nm. The inset in (b) shows a magnification of the 620 nm data.

relatively long lifetime (6.36 ns in toluene, 5.35 ns in chlorobenzene, and 5.50 ns in dichloromethane) due to some rest emission from PDI, $(PDI)_n$, or an impurity and a large component (~99%) with a short emission lifetime that shows the (quenched) emission of nonaggregated PDI, which is quenched faster with increasing solvent polarity (290 ps in toluene, 150 ps in chlorobenzene, and 90 ps in dichloromethane). The latter shows that the emission of the nonaggregated PDI moieties in PFP−PDI is effectively quenched compared to the reference dialkyl-PDI. The possible explanations of this quenching are (1) energy transfer to aggregated PDI species or (2) electron transfer by accepting an electron from the PFP backbone.

As it has been shown, PDI aggregates ($(PDI)_n$) show an emission maximum at 620 nm (Figure 5). The emission at this wavelength consists of a long (61.7% in toluene, 53.7% in chlorobenzene, and 45.9% in dichloromethane) and a short-lived component. The inset of Figure 7b shows a magnification of the first 2 ns, disclosing the short-lived component. The long-lived component is longer than that of the nonaggregated PDI emission, which is typical for aggregated PDI. Previously, lifetimes of 15−23 ns have been reported for PDI excimer emission.[38,46b,64] The photoluminescence lifetime of the long-lived component decreases when going from toluene (11.3 ns) to chlorobenzene (9.29 ns) and dichloromethane (5.54 ns). An explanation for this reduction in lifetime can be that the aggregates are less tightly packed in more polar solvents and that the excitations are thus less delocalized in those solvents, which increases the decay rate to the ground state. Another explanation for the shorter lifetimes is that electron transfer from the aggregates takes place. In more polar solvents this process can occur faster because the driving force for electron transfer (ΔG_{CS}) from the aggregates (with an energy of around 1.95 eV) is larger due to the stabilization of the charge separated state by the higher polarity of the solvent. The short-lived component of the photoluminescence emission at 620 nm also shows a reduction in lifetime with increasing solvent polarity: from 540 ps in toluene to 260 ps in chlorobenzene and 175 ps in dichloromethane.

So far, the experimental results have shown that energy transfer takes place from PFP to nonaggregated PDI and mostly to aggregated PDI moieties, which emit only a little because of their stacking. However, another explanation is required to explain the full set of data. As we have seen, part of the nonaggregated PDI moieties decay by a different mechanism, as the excitation spectrum at 630 nm lacks a considerable amount of absorption at 530 nm. An extra decay process could be electron transfer in competition with the energy transfer process from PFP to nonaggregated PDI. This would also explain the shorter lifetimes of the nonaggregated PDI emission when more polar solvents are used. The reduction in lifetime that follows from the 620 nm emission can also be due to electron transfer from the PFP to the PDI aggregates. The short component in the 620 nm emission can be due to electron transfer from the nonaggregated PDI.

Electron Transfer: Weller Equation. In order to find out whether electron transfer is a likely process for PFP−PDI, we can use the Weller equation (1).[65] We can use the oxidation potential (+0.56 eV vs Fc/Fc^+) and the reduction potential (−0.98 eV vs Fc/Fc^+) of PFP−PDI and the energy of the lowest excited singlet state, S_1, of the nonaggregated PDI moieties (2.32 eV in toluene) to predict the Gibbs free energy for electron transfer from the PFP backbone to the PDI moieties on the basis of the Weller equation:

$$\Delta G_{CS} = -e[E_{ox}(D) - E_{red}(A)] + E(S_1) + \frac{e^2}{4\pi\epsilon_0\epsilon_s R_{cc}} + \frac{e^2}{8\pi\epsilon_0}\left(\frac{1}{r^+} + \frac{1}{r^-}\right)\left(\frac{1}{\epsilon_{ref}} - \frac{1}{\epsilon_s}\right) \quad (1)$$

The radius of the PFP radical cation and the PDI radical anion were set to $r^+ = 5.0$ Å and $r^- = 4.7$ Å, respectively, whereas the center-to-center chromophore distance (R_{cc}) was set at 20 Å, which is the maximum distance that can be reached.[63] The resulting values for ΔG_{CS} (Table 3) predict that electron transfer from the nonaggregated PDI moieties is energetically favorable in all the solvents investigated, with the lowest driving force for the less polar toluene (−0.16 eV). We note that electron transfer is more favorable if the PDI units are closer than the maximum distance of 20 Å. Electron transfer to the PDI aggregates is less probable in toluene, as the energy of the lowest excited-state of the aggregated PDI is ∼1.95 eV (the maximum of the emission). If a value of 1.95 eV is used for $E(S_1)$ of $(PDI)_n$ in eq 1, ΔG_{CS} would be −0.34 eV for chlorobenzene and −0.48 eV for dichloromethane. So, from eq 1 it seems likely that electron transfer is a competing process for energy transfer from PFP to PDI or $(PDI)_n$ and for energy transfer from PDI to $(PDI)_n$ in chlorobenzene and dichloromethane.

For toluene $\Delta G_{CS} = +0.21$ eV from $(PDI)_n$. In the calculations we have used the relative permittivity ($\epsilon_r = 2.43$) for toluene, which results in a value of $E_{CS} = 2.15$ eV. However, for solvents like toluene that have a low dipole moment and a high quadrupole moment, the bulk relative permittivity underestimates the local dipolar character.[66] When a value of the "effective" relative permittivity, $\epsilon_{eff} = 3.5$, is used in eq 1, a value of $E_{CS} = 1.85$ eV is found.[67] Thus, electron transfer to $(PDI)_n$ (with an energy of $E(S_1) = 1.95$ eV) can then also be anticipated.

Temperature-Dependent Measurements. Additional evidence showing the presence of intramolecular PDI aggregates in PFP−PDI comes from the concentration- and temperature-dependent absorption and emission spectra. Figure 8a shows that the absorption spectra of PFP−PDI in chlorobenzene are independent of the concentration in the range of 10^{-4}−10^{-6} M (monomer units), consistent with intramolecular aggregation. At higher temperatures it is expected that aggregates dissociate, resulting in absorption and emission spectra more similar to those of nonaggregated PDI. In Figure 8 it is shown that this is indeed observed: when a solution of PFP−PDI in chlorobenzene is heated, the absorption spectrum gradually matches the nonaggregated PDI absorption spectrum shown in Figure 4. Thus, the peak of the (0,0) vibration increases, and the peaks corresponding to the (0,1) and (0,2) vibrations of PDI reduce in intensity upon heating (Figure 8b). The tailing into the red also becomes less, gradually resembling the absorption spectrum of the reference dialkyl-PDI. However, even at 90 °C a considerable amount of aggregation still remains, as the ratio between the (0,0) and the (0,1) vibration peaks is only 1.27, lower than the value of 1.62 observed for the nonaggregated reference dialkyl-PDI. The temperature-dependent photoluminescence shows the same trend: from 10 to 100 °C the emission from the aggregates (at 630 nm) gradually decreases in intensity (Figure 8c) and the emission at 535 nm (nonaggregated PDI) increases, but even at 100 °C there is still some remaining emission from stacked PDI groups. It is important to note that the changes were completely reversible upon cooling back to 10 °C.

These measurements provide an extra indication for electron transfer to nonaggregated PDI: on going from 10 to 100 °C the photoluminescence intensity of aggregated PDI is reduced by a factor of 5.8, whereas the photoluminescence intensity of nonaggregated PDI (at 535 nm) is increased only by a factor of 1.3. The explanation for this mismatch is that the increasing amount of nonaggregated PDI molecules is compensated for by an increased electron transfer from PFP to PDI. The fact that upon heating the PFP emission (at 410 nm) is further reduced by a factor 1.6 supports the idea that extra electron transfer from PFP to PDI takes place if the PDI are no longer in the aggregated state.

The photoluminescence lifetime of the aggregate emission (probed at 640 nm) is also reduced with increasing temperature (Figure 8d). Again, reversibility of the changes upon cooling was observed. Thus, it seems that electron transfer also takes place to the stacked PDI groups. For this electron transfer an activation barrier is present that is overcome at higher temperature. An alternative explanation for the shorter lifetime at higher temperature is that at high temperature the H-aggregates are less tightly packed, which allows structural deformation to a configuration that couples radiatively to the ground state. This effect would reduce the PL lifetime and increase the PL quantum yield. Since the latter is not the observed, we favor an interpretation in terms of electron transfer. Transient absorption spectroscopy in the nanosecond domain on PFP−PDI in solution, however, failed to provide conclusive evidence for the expected formation of PFP cations or PDI anions. Although this experiment itself does not strengthen our conclusions, we note that intramolecular recombination can be very fast (<100 ps) such that the formed charges cannot be detected.[68]

The results of the measurements in solution can be summarized in a Jablonski diagram (Figure 9). After excitation of the PFP, the emission from that state is quenched by energy and electron transfer to PDI. From the nonaggregated PDI the photoluminescence emission is also quenched, by energy transfer to aggregated PDI ($(PDI)_n$) and also by electron transfer by accepting an electron from PFP. The latter process is favored by using a more polar solvent or at higher temperature.

Measurements in the Solid State. In parallel to the investigation of PFP−PDI in solution, thin films of PFP−PDI have also been studied. The absorption spectrum of a thin film of PFP−PDI spin-cast from chlorobenzene is shown in Figure 10. The film shows even more evidence of aggregation than PFP−PDI in toluene solutions, as the ratio between the peaks of the (0,0) and the (0,1) vibrations is now only 0.80. The photoluminescence spectrum reveals only minimal emission, as it could be expected from an aggregated film in which electron transfer takes place.

Direct evidence for electron transfer in a thin film comes from photoinduced absorption (PIA) spectroscopy recorded at 80 K. The dashed line in Figure 11 shows the PIA spectrum of the reference polymer PFP in a thin film, displaying a maximum at 1.56 eV and a shoulder toward higher energy. This absorption can be assigned to the triplet−triplet absorption of the polymer. In dichloromethane a similar spectrum was measured but blue-shifted compared to the film with a maximum of the triplet−triplet absorption at 1.70 eV. A triplet−triplet absorption of a PFP in benzene has been recently reported, also showing a maximum at 1.70 eV.[69] The PIA spectrum of a PFP−PDI film at 80 K is also shown in Figure 11 (solid line) and clearly exhibits the characteristic absorption of $PDI^{\bullet-}$ with maxima at 1.72, 1.54, and 1.28 eV.[70] The positions of the $PFP^{\bullet+}$ cation bands are less clear. As for other conjugated polymers like MEH−PPV[71] and P3HT,[72] $PFP^{\bullet+}$ is expected to have a low- and high-energy absorption band. The position of the high-energy band was previously reported to be at 2.3 eV; however,

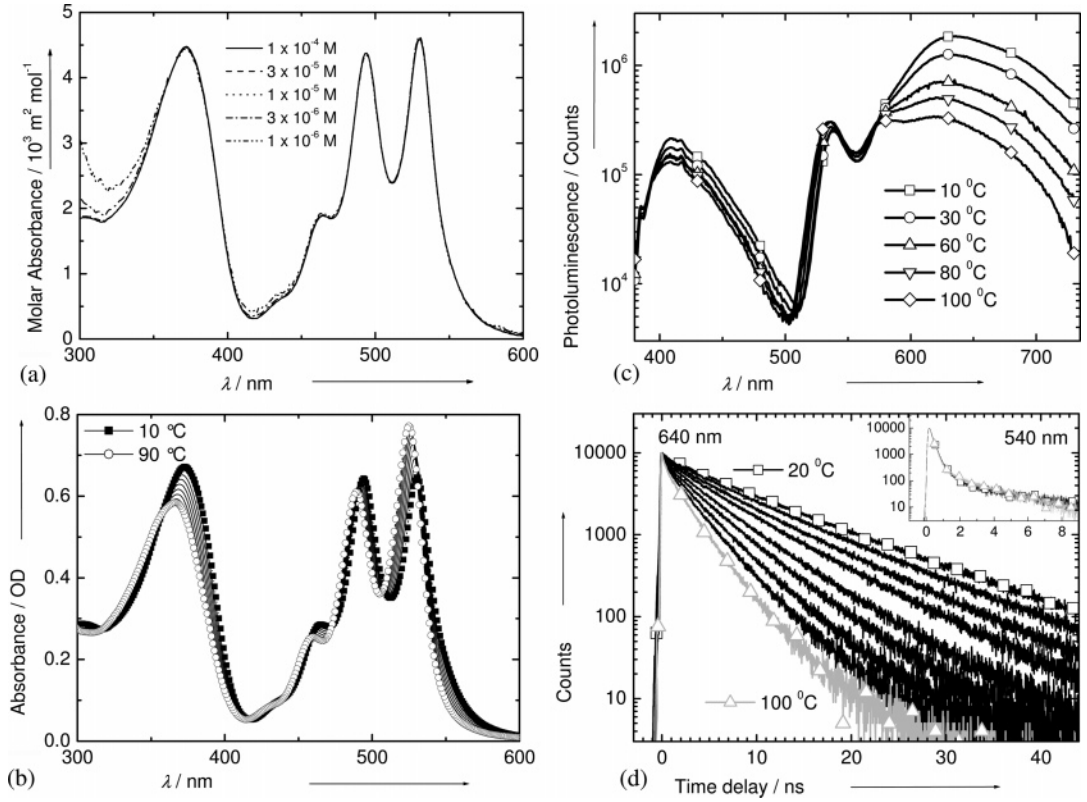

Figure 8. (a) Concentration-dependent absorption spectra of PFP−PDI in chlorobenzene. (b, c, d) Spectral temperature dependence of a solution of PFP−PDI in chlorobenzene: (b) absorption spectra, (c) photoluminescence spectra, and (d) time-resolved photoluminescence lifetime spectra at 640 nm. The inset shows the effect of increasing the temperature at 540 nm.

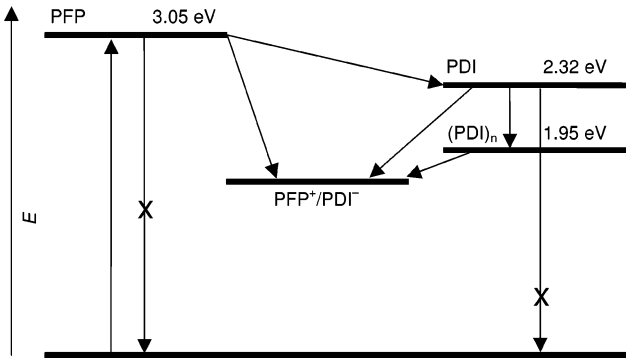

Figure 9. Energy level diagram showing the lowest excited singlet states of PFP and nonaggregated PDI, of the PDI aggregates $(PDI)_n$, and that of the charge-separated state between PFP and PDI. The energy of the charge-separated state is affected by the polarity of the solvent (see text). The arrows (without the crosses) show the main processes that occur upon photoexcitation of PFP.

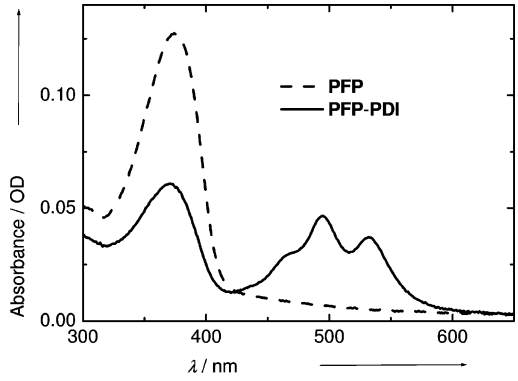

Figure 10. Absorption spectra at 295 K of thin films of PFP and PFP−PDI spin-cast from chlorobenzene.

the position of the low-energy band remains unclear.[73] Two bands are visible at low energy in our spectrum: one at 1.10 eV and a possible band with an onset at around 0.5 eV. To identify the position of the low-energy band, we conducted a separate experiment. Thus, a PIA spectrum of PFP was taken in a mixed film with a fullerene derivative (PCBM). This revealed peaks of $PFP^{\bullet+}$ at 0.5 and 2.4 eV, together with that of the PCBM radical anion at 1.24 eV. Thus, for PFP−PDI we tentatively assign the band at 0.5 eV to the $PFP^{\bullet+}$ low-energy band. Presently, we have no consistent explanation for the peak at 1.1 eV.

At an energy above 2.1 eV the bleaching bands of PDI are present, at 2.22, 2.48, and 2.68 eV. Interestingly, another feature with a strong absorption is present in this region, resulting in a peak at 2.36 eV. Likely, this is due to a triplet−triplet absorption of the PDI moieties.[44a] The energy of the lowest excited triplet state for nonaggregated PDI is at 1.2 eV [44a] (and for aggregated PDI presumably even lower), making charge recombination of photoinduced charges (with an energy of ~1.55 eV, from E_{ox}-(D) − E_{red}(A)) into the triplet excited state of the PDI a possible decay route.

Conclusions. In this paper we have described the synthesis of the structurally well-defined PFP−PDI polymer, in which a poly(fluorene-*alt*-phenylene) (PFP) chain is functionalized with PDI units as pendant groups. The synthetic approach allows for the introduction of a high number of PDI electron acceptor units, making possible and facilitating the formation of PDI aggregates within the polymeric chain itself. Moreover, the selective choice of the monomeric units allows tailoring the electron-donating ability of the polymer backbone, thus enabling photoinduced electron transfer. In fact, the cyclic voltammetry data of PFP−PDI shows amphoteric behavior, combining the good acceptor properties of PDI with the good electron donor ability of the PFP backbone. UV−vis absorption, steady-state

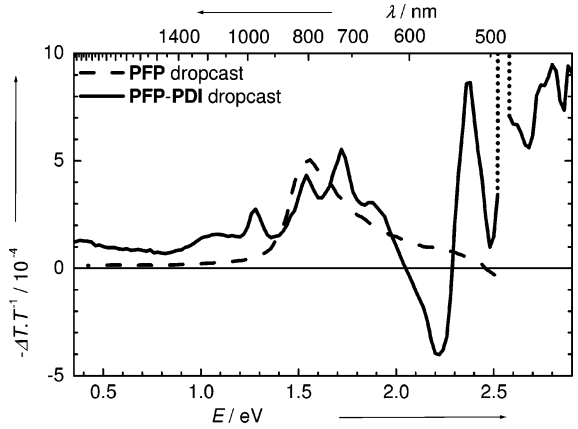

Figure 11. Photoinduced absorption spectra of thin films of PFP (dashed line) and PFP−PDI (solid line) on a quartz plate at 80 K. The dotted peak in the PFP−PDI spectrum at 2.54 eV is due to the laser.

fluorescence, and excitation spectroscopy point to the existence of PDI aggregates in different solvents, which is further confirmed by temperature-dependent studies. Solvent and temperature-dependent studies, together with the analysis of photoluminescence lifetimes, evidence the existence of photoinduced electron transfer from the electron-donating poly(fluorene-*alt*-phenylene) chain not only to the electron-accepting PDI pendant units but also, and more remarkably, to PDI aggregates. PIA measurements corroborate these results and indicate that electron transfer also occurs in the solid state. Work is in progress in order to further control and optimize the extension of these processes by the introduction of different spacers and comonomers.

Experimental Section

Materials. 4-(Hexyloxy)-2,5-diiodophenol (**7**),[49] *N*-(4-hydroxyphenyl)-*N*′-(10-nonadecyl)perylene-3,4:9,10-bis(dicarboximide) (**11**),[50] 2,7-bis(4,4,5,5-tetramethyl-1,3,2-dioxaborolan-2-yl)-9,9-(3,7-dimethyloctyl)fluorene (**13**),[51] 1,4-dihexyloxy-2,5-diiodobenzene (**14**),[53] 2,7-bis(4,4,5,5-tetramethyl-1,3,2-dioxaborolan-2-yl)-9,9-dihexylfluorene (**15**),[54] and *N*,*N*′-(1-hexylheptyl)perylene-3,4:9,10-bis(dicarboximide) (dialkyl-PDI)[56] were prepared following previously reported synthetic procedures. Dialkyl-PDI was carefully purified using column chromatography.[74] All other chemicals were purchased from Aldrich and used as received without further purification unless otherwise specified. Column chromatography was performed on Merck Kieselgel 60 silica gel (230−240 mesh). Thin layer chromatography was carried out on Merck silica gel F-254 flexible TLC plates. Solvents and reagents were dried by usual methods prior to use and typically used under inert gas atmosphere.

Characterization. Melting points were measured with an Electrothermal melting point apparatus and are uncorrected. FTIR spectra were recorded as KBr pellets in a Shimadzu FTIR 8300 spectrometer. NMR were recorded on a Bruker AC-200, Avance 300, or AMX-400 apparatus as noted, and the chemical shifts were reported relative to tetramethylsilane (TMS) at 0.0 ppm (for ^{1}H NMR) and $CDCl_3$ at 77.16 ppm (for ^{13}C NMR). The splitting patterns are designated as follows: s (singlet), d (doublet), m (multiplet), and b (broad), and the assignments are Pery (PDI) and Ph (phenyl) for ^{1}H NMR. Mass spectra were recorded with a Varian Saturn 2000 GC-MS and with a MALDI-TOF MS Bruker Reflex 2 (dithranol as matrix). Elemental analyses were performed on a Perkin-Elmer EA 2400.

Electrochemistry. Cyclic voltammetry experiments were performed with a computer-controlled EG & G PAR 273 potentiostat in a three-electrode single-compartment cell (5 mL). The platinum working electrode consisted of a platinum wire sealed in a soft glass tube with a surface of $A = 0.785$ mm^2, which was polished down to 0.5 μm with Buehler polishing paste prior to use in order to obtain reproducible surfaces. The counter electrode consisted of a platinum wire, and the reference electrode was a Ag/AgCl secondary electrode. All potentials were internally referenced to the ferrocene−ferrocenium couple. For the measurements, concentrations of 5×10^{-3} mol L^{-1} of the electroactive species were used in freshly distilled and deaerated dichloromethane (Lichrosolv, Merck) and 0.1 M tetrabutylammonium hexafluorophosphate ($TBAPF_6$, Fluka) which was twice recrystallized from ethanol and dried under vacuum prior to use.

Absorption and Fluorescence. UV−vis absorption spectra were recorded using a Perkin-Elmer Lambda 900 spectrophotometer, and steady-state fluorescence spectra were recorded on an Edinburgh Instruments FS920 double-monochromator spectrophotometer with a Peltier-cooled red-sensitive photomultiplier. The emission spectra were not corrected for the wavelength dependence of the sensitivity of the detection system. Time-correlated single photon counting fluorescence studies were performed on an Edinburgh Instruments LifeSpec-PS spectrometer by photoexcitation with a 400 nm picosecond laser (PicoQuant PDL 800B) operated at 2.5 MHz and detection with a Peltier-cooled Hamamatsu microchannel plate photomultiplier (R3809U-50).

Photoinduced Absorption. Near-steady-state photoinduced absorption (PIA) spectra were recorded between 0.40 and 3.0 eV by excitation with a mechanically modulated CW argon ion laser (488 nm, 275 Hz) pump beam and measuring the change in transmission of a tungsten−halogen probe beam through the sample (ΔT) with a phase-sensitive lock-in amplifier after detection using Si, InGaAs, and cooled InSb detectors. The pump power was typically 50 mW with a beam diameter of 2 mm. The PIA signal ($-\Delta T T^{-1}$) was corrected for the photoluminescence, which was recorded in a separate experiment. Samples of drop-cast thin films were held at 80 K in an inert nitrogen atmosphere using an Oxford Optistat continuous flow cryostat. Samples in solution were prepared in inert atmosphere and measured in a 1 mm Spectrocell quartz cuvette with an airtight screw cap.

1-(6′-Chlorohexyloxy)-4-hexyloxy-2,5-diiodobenzene (9). Under an argon atmosphere, a mixture of 4-(hexyloxy)-2,5-diiodophenol (**7**) (900 mg, 2.0 mmol), potassium carbonate (552 mg, 4.0 mmol), and 1-bromo-6-chlorohexane (**8**) (798 mg, 4.0 mmol) in 60 mL of dry DMF was heated at 100 °C. After 48 h, the reaction mixture was allowed to cool to room temperature and poured into a 1 M HCl aqueous solution. The mixture was then extracted with dichloromethane, and the combined organic extracts were dried over $MgSO_4$ and evaporated under vacuum. The remaining oil was purified by column chromatography (silica gel, hexanes/dichloromethane 1/1) to give 1-(6′-chlorohexyloxy)-4-hexyloxy-2,5-diiodobenzene (**9**) as a colorless solid (72%); mp 40−41 °C (hexanes/dichloromethane). ^{1}H NMR ($CDCl_3$, 200 MHz): $\delta = 7.17$ (s, 2H, Ph), 3.94 (t, 2H, $J = 6.2$ Hz, $-OCH_2$), 3.93 (t, 2H, $J = 6.4$ Hz, $-OCH_2$), 3.56 (t, 2H, $J = 6.6$ Hz, $-CH_2Cl$), 1.91−1.73 (m, 6H, $-CH_2-$), 1.56−1.45 (m, 6H, $-CH_2-$), 1.37−1.34 (m, 4H, $-CH_2-$), 0.91 (t, 3H, $J = 6.7$ Hz, $-CH_3$). ^{13}C NMR ($CDCl_3$, 50 MHz): $\delta = 152.90$ ($C_{Ar}-O$), 152.73 ($C_{Ar}-O$), 122.80 (C_{Ar}), 122.78 (C_{Ar}), 86.30 ($C_{Ar}-I$), 86.28 ($C_{Ar}-I$), 70.36 ($-OCH_2$), 70.06 ($-OCH_2$), 44.98 ($-CH_2Cl$), 32.50, 31.45, 29.10, 28.98, 26.54, 25.70, 25.42, 22.57, 14.02 ($-CH_3$). MS (EI) (*m*/*z*, % int): 564 (M^+, 41), 480 (14), 362 (100), 83 (29), 55 (44), 43 (46). FTIR (KBr, cm^{-1}): $\nu = 2939$, 2866, 1636, 1489, 1466, 1350, 1265, 1211, 1057, 1022, 798, 725. Microanalysis: Calcd for $C_{18}H_{27}ClI_2O_2$: C: 38.29%; H: 4.82%. Found: C: 38.19%; H: 4.79%.

1-Hexyloxy-2,5-diiodo-4-(6′-iodohexyloxy)benzene (10). 1-(6′-Chlorohexyloxy)-4-hexyloxy-2,5-diiodobenzene (**9**) (865 mg, 1.53 mmol) and NaI (459 mg, 3.06 mmol) were dissolved in 50 mL of dry acetone and heated at reflux for 48 h. After cooling to room temperature, the precipitated NaCl was filtered off and the solvent evaporated under vacuum. The residue was then dissolved in dichloromethane and washed with water. The organic phase was dried over $MgSO_4$, and the solvent evaporated under vacuum to give 1-hexyloxy-2,5-diiodo-4-(6′-iodohexyloxy)benzene (**10**) as a colorless solid (92%) with enough analytical purity to be used

without any further purification; mp 35−36 °C (dichloromethane). ^{1}H NMR ($CDCl_3$, 200 MHz): δ = 7.17 (s, 2H, Ph), 3.94 (t, 2H, J = 6.2 Hz, $-OCH_2$), 3.93 (t, 2H, J = 6.4 Hz, $-OCH_2$), 3.22 (t, 2H, J = 7.0 Hz, $-CH_2I$), 1.94−1.73 (m, 6H, $-CH_2-$), 1.57−1.49 (m, 6H, $-CH_2-$), 1.37−1.34 (m, 4H, $-CH_2-$), 0.91 (t, 3H, J = 6.7 Hz, $-CH_3$). ^{13}C NMR ($CDCl_3$, 50 MHz): δ = 152.90 ($C_{Ar}-O$), 152.73 ($C_{Ar}-O$), 122.80 (C_{Ar}), 122.78 (C_{Ar}), 86.30 ($C_{Ar}-I$), 86.28 ($C_{Ar}-I$), 70.37 ($-OCH_2$), 70.06 ($-OCH_2$), 33.38, 31.46, 30.12, 29.10, 28.93, 25.70, 25.06, 22.58, 14.03 ($-CH_3$), 6.96 ($-CH_2I$). MS (EI) (m/z, % int): 656 (M^+, 25), 572 (4), 362 (100), 83 (34), 55 (39), 43 (39). FTIR (KBr, cm^{-1}): ν = 2936, 2851, 1639, 1485 1465 1350, 1265, 1211, 1057, 1022, 798, 725. Microanalysis: Calcd for $C_{18}H_{27}I_3O_2$: C: 32.95%; H: 4.15%. Found: C: 33.06%; H: 4.22%.

Monomer 12. To a solution of *N*-(4-hydroxyphenyl)-*N*′-(10-nonadecyl)perylene-3,4:9,10-bis(dicarboximide) (**11**) (180 mg, 0.24 mmol) in 50 mL of anhydrous DMF, potassium carbonate (66 mg, 0.48 mmol), and 1-hexyloxy-2,5-diiodo-4-(6′-iodohexyloxy)benzene (**10**) (157 mg, 0.24 mmol) were added under an argon atmosphere. The mixture was heated at reflux for 48 h. The crude was allowed to reach room temperature and treated with a 1 M HCl aqueous solution. The resulting mixture was extracted with dichloromethane, and the combined organic fractions were dried over $MgSO_4$ and evaporated under vacuum. The remaining residue was purified by column chromatography (silica gel, hexanes/dichloromethane 2/8) to give monomer **12** as a deep red solid (37%); mp >300 °C. ^{1}H NMR ($CDCl_3$, 200 MHz): δ = 8.75 (d, 2H, Pery), 8.69−8.64 (m, 6H, Pery), 7.26−7.18 (m, 4H, Ph), 7.08 (d, J = 8.8 Hz, 2H, Ph), 5.20 (bs, 1H, −N−CH), 4.06 (t, 2H, J = 6.3 Hz, $-OCH_2-$), 4.00−3.90 (m, 4H, $-OCH_2-$), 1.95−1.77 (m, 8H, $-CH_2-$), 1.65−1.50 (m, 10H, $-CH_2-$), 1.40−1.15 (m, 30H, $-CH_2-$), 0.95−0.77 (m, 9H, $-CH_3$). ^{13}C NMR ($CDCl_3$, 50 MHz): δ = 163.78, 159.26 ($C_{Ar}-O$), 152.93 ($C_{Ar}-O$), 135.00, 134.98, 134.32, 131.94, 131.82, 131.78, 129.77, 129.76, 129.53, 127.30, 126.39, 123.46, 123.43, 123.39, 123.28, 123.27, 123.24, 115.28, 86.33 ($C_{Ar}-I$), 70.37 ($-OCH_2$), 70.19 ($-OCH_2$), 68.07 ($-OCH_2$), 54.83 (−N−CH), 32.37, 31.85, 31.47, 29.54, 29.27, 29.12, 26.98, 25.71, 22.64, 14.08. MS (FAB) (m/z): 1278.8 ($M^+ + 1$). FTIR (KBr, cm^{-1}): ν = 2921, 2852, 1695, 1651, 1593, 1577, 1509, 1485, 1463, 1465, 1343, 1249, 1208, 1174, 810, 746. Microanalysis: Calcd for $C_{67}H_{78}I_2N_2O_7$: C: 63.00%; H: 6.15%; N: 2.19%. Found: C: 62.63, %; H: 6.00%; N: 2.06%.

Polymer PFP−PDI. A solution of monomer **12** (80 mg, 0.06 mmol), 2,7-bis(4,4,5,5-tetramethyl-1,3,2-dioxaborolan-2-yl)-9,9-(3,7-dimethyloctyl)fluorene (**13**) (43 mg, 0.06 mmol), and tetrakis-(triphenylphosphine)palladium(0) (1 mg, 1 × 10^{-3} mmol) in a deareated mixture of 12 mL of dry THF and 10 mL of an aqueous potassium carbonate 2 M solution is heated at reflux under argon atmosphere for 48 h. The thick reaction mixture is allowed to cool to room temperature, and methanol is added to give an abundant red precipitate. The solid is collected, dissolved in chloroform, and precipitated out of methanol. The solid is collected by centrifugation and thoroughly washed with methanol and diethyl ether to give PFP−PDI as a bright red solid (98%). ^{1}H NMR ($CDCl_3$, 400 MHz): δ = 8.73−8.45 (bm, 8H, Pery), 8.35−8.25 (m, 2H), 7.82−7.63 (m, 8H), 7.13−7.06 (m, 2H), 5.12 (b, 1H, -N−CH), 4.06 (bs, 6H, $-OCH_2$), 2.27 (bs, 4H, $-CH_2-$), 1.80 (bs, 4H, $-CH_2-$), 1.56 (bs, 12H, $-CH_2-$), 1.21 (bs, 24H, $-CH_2-$) 1.04 (bs, 8H, $-CH_2-$), 0.79 (bs, 27H, $-CH_3$). FTIR (KBr, cm^{-1}): ν = 2923, 2854, 1699, 1653, 1594, 1578, 1509, 1462, 1342, 1251, 1208, 810, 746. Microanalysis: Calcd for $[C_{98}H_{126}N_2O_7]_n$: C: 81.81%; H: 8.79%; N: 1.94%. Found: C: 81.57, %; H: 8.44%; N: 1.83%. SEC (vs PS): M_n: 101 000 g/mol; M_w: 16 400 g/mol; pd: 6.2.

Polymer PFP. A solution of 1,4-dihexyloxy-2,5-diiodobenzene (**14**) (53 mg, 1.0 mmol), 2,7-bis(4,4,5,5-tetramethyl-1,3,2-dioxaborolan-2-yl)-9,9-dihexylfluorene (**15**) (58 mg, 1.0 mmol), and tetrakis(triphenylphosphine)palladium(0) (17 mg, 15 × 10^{-3} mmol) in a deareated mixture of 10 mL of dry THF and 8 mL of an aqueous potassium carbonate 2 M solution is heated at reflux under argon atmosphere for 48 h. The reaction mixture is allowed to cool to room temperature, and methanol is added to give an off-yellow precipitate. The solid is collected, dissolved in chloroform, and precipitated out of methanol. The solid is collected by centrifugation and thoroughly washed with methanol and diethyl ether to give PFP as a beige solid (92%). ^{1}H NMR ($CDCl_3$, 400 MHz): δ = 7.79−7.59 (m, 6H), 7.26−7.13 (m, 2H), 3.97 (bs, 4H, $-OCH_2-$), 2.05 (bs, 4H), 1.73 (bs, 8H, $-CH_2-$), 1.53−1.09 (m, 20H), 0.87−0.78 (m, 12H). ^{13}C NMR ($CDCl_3$, 100 MHz): δ = 150.48 ($C_{Ar}-O$), 139.85, 137.04, 135.00, 131.29, 127.95, 127.52, 124.43, 119.22, 116.80, 69.91 ($-OCH_2$), 55.06 ($_{bridge}$), 40.61 ($C_{bridge}-CH_2$), 31.51, 29.99, 29.46, 25.78, 24.32, 22.66, 14.01. FTIR (KBr, cm^{-1}): ν = 2953, 2927, 2856, 1509, 1461, 1435, 1377, 1203, 821. Microanalysis: Calcd for $[C_{43}H_{60}O_2]_n$: C: 84.81%; H: 9.93%. Found: C: 84.67, %; H: 9.92%. SEC (vs PS): M_n: 38 000 g/mol; M_w: 13 100 g/mol; pd: 2.9.

Acknowledgment. We thank R. Abbel for kindly providing a first batch of initial starting materials and Dr. S. Chopin for a gift of dialkyl-PDI. We also thank the MCyT (Ref CTQ2004-03760) and Comunidad de Madrid (PR45/05-14167) and the Universidad Complutense de Madrid (PR1/07-14894) for financial support. R.G. is indebted to the "Programa Ramón y Cajal" and the Flores Valles Company. R.B thanks the Comunidad de Madrid for a doctoral fellowship. The research has been also financially supported by the NAIMO EU integrated project (NMP4-CT-2004-500355).

References and Notes

(1) (a) *Organic Light-Emitting Devices*; Müllen, K., Scherf, U., Eds.; Wiley-VCH: Weinheim, 2006. (b) *Organic Electroluminescence*; Kafafi, Z. H., Ed.; Taylor & Francis: London, 2005. (c) *Organic Light-Emitting Devices*; Shinar, J., Ed.; Springer-Verlag: New York, 2003.

(2) (a) *Organic Photovoltaics. Concepts and Realization;* Brabec, C. J., Dyakonov, V., Parisi, J., Sariciftci, N. S., Eds.; Springer-Verlag: Berlin, 2003. (b) Gómez, R.; Segura, J. L. In *Handbook of Organic Electronic and Photonics*; Nalwa, H. S., Ed.; American Scientific Publishers: Valencia, CA, in press.

(3) (a) Kraft, A.; Grimsdale, A. C.; Holmes, A. B. *Angew. Chem., Int. Ed.* **1998**, *37*, 402. (b) Mitschke, U.; Bäuerle, P. *J. Mater. Chem.* **2000**, *10*, 1471. (c) Ackelrud, L. *Prog. Polym. Sci.* **2003**, *28*, 875.

(4) Peumans, P.; Yakimov, A.; Forrest, S. R. *J. Appl. Phys.* **2003**, *93*, 3693.

(5) Schmidt-Mencke, L.; Fechtenkötter, A.; Müllen, K.; Moons, E.; Friend, R. H.; MacKenzie, J. D. *Science* **2001**, *293*, 1119.

(6) (a) Tang, H.-Z.; Fujiki, M.; Zhang, Z.-B.; Torimitsu, K.; Motonaga, M. *Chem. Commun.* **2001**, 2426. (b) Lee, J.-H.; Hwang, D.-H. *Chem. Commun.* **2003**, 2836. (c) Wu, F.-I.; Dodda, R.; Huang, K. J.-H.; Hsu, C.-S.; Shu, C.-F. *Polymer* **2004**, *45*, 4257. (d) Su, H.-J.; Wu, F.-I.; Tseng, Y.-H.; Shu, C.-F. *Adv. Funct. Mater.* **2005**, *15*, 1209. (e) Knaapila, M.; Stepanyan, R.; Lyons, B. P.; Tokkeli, M.; Monkman, A. P. *Adv. Funct. Mater.* **2006**, *16*, 599.

(7) (a) Ego, C.; Grimsdale, A. C.; Uckert, F.; Yu, G.; Srdanov, V. I.; Müllen, K. *Adv. Mater.* **2002**, *14*, 809. (b) Pogantsch, A.; Wenzl, F. P.; List, E. J. W.; Leising, G.; Grimsdale, A. C.; Müllen, K. *Adv. Mater.* **2002**, *14*, 1061.

(8) (a) Zollinger, H. In *Color Chemistry*, 3rd ed.; VCH: Weinheim, 2003. (b) Herbst, W.; Hunger, K. In *Industrial Organic Pigments: Production, Properties, Applications*, 2nd ed.; Wiley-VCH: Weinheim, 1997.

(9) (a) Struijk, C. W.; Sieval, A. B.; Dakhorst, J. E. J.; van Dijk, M.; Kimkes, P.; Koehorst, R. B. M.; Donker, H.; Schaafsma, T. J.; Picken, S. J.; van de Craats, A. M.; Warman, J. M.; Zuilhof, H.; Sudhölter, E. J. R. *J. Am. Chem. Soc.* **2000**, *122*, 11057. (b) Dimitrakopoulos, C. D.; Malenfant, P. R. L. *Adv. Mater.* **2002**, *14*, 99.

(10) (a) Halls, J. J. M.; Friend, R. H. *Synth. Met.* **1997**, *85*, 1307. (b) Petrisch, K.; Dittmer, J. J.; Marseglia, E. A.; Friend, R. H.; Lux, A.; Rozenberg, G. G.; Moratti, S. C.; Holmes, A. B. *Sol. Energy Mater. Sol. Cells* **2000**, *61*, 63. (c) Breeze, A. J.; Salomon, A.; Ginley, D. S.; Gregg, B. A.; Tillmann, H.; Hörhold, H.-H. *Appl. Phys. Lett.* **2002**, *81*, 3085. (d) Yakimov, A.; Forrest, S. R. *Appl. Phys. Lett.* **2002**, *80*, 1667. (e) Im, C.; Bässler, H.; Fechtenkötter, A.; Watson, M. D.; Müllen, K. *Synth. Met.* **2003**, *139*, 683.

(11) (a) Malenfant, P. R. L.; Dimitrakopoulos, C. D.; Gelorme, J. D.; Kosbar, L. L.; Graham, T. O.; Curioni, A.; Andreoini, W. *Appl. Phys. Lett.* **2002**, *80*, 2517. (b) Chesterfield, R. J.; Mckeen, J. C.; Newman, C. R.; Frisbie, C. D. *J. Appl. Phys.* **2004**, *95*, 6396. (c) Rost, C.; Gundlach, D. J.; Karg, S.; Riess, W. *J. Appl. Phys.* **2004**, *95*, 5782.

(12) Süssmeier, F.; Langhals, H. *Eur. J. Org. Chem.* **2001**, 607.

(13) (a) He, X.; Liu, H.; Li, Y.; Wang, S.; Wang, N.; Xiao, J.; Xu, X.; Zhu, D. *Adv. Mater.* **2005**, *17*, 2811. (b) Zang, L.; Liu, R.; Holman, M. W.; Nguyen, K. T.; Adams, D. M. *J. Am. Chem. Soc.* **2002**, *124*, 10640.

(14) Yukruk, F.; Dogan, A. L.; Canpinar, H.; Guc, D.; Akkaya, E. U. *Org. Lett.* **2005**, *7*, 2885.

(15) Ego, C.; Marsitzky, D.; Becker, S.; Zhang, J.; Grimsdale, A. C.; Müllen, K.; Mackenzie, J. D.; Silva, C.; Friend, R. H. *J. Am. Chem. Soc.* **2003**, *125*, 437.

(16) (a) Langhals, H.; Jaschke, H.; Ring, U.; von Unold, P. *Angew. Chem.* **1999**, *111*, 143; *Angew. Chem., Int. Ed.* **1999**, *38*, 201. (b) Rohr, U.; Kohl, C.; Müllen, K.; van de Craats, A.; Warman, J. *J. Mater. Chem.* **2001**, *11*, 1789. (c) Adachi, M.; Nagao, Y. *Chem. Mater.* **2001**, *13*, 662. (d) Tam-Chang, S.-W.; Seo, W.; Iverson, I. K.; Casey, S. M. *Angew. Chem., Int. Ed.* **2003**, *42*, 897. (e) Nolde, F.; Qu; J.; Kohl, C.; Pschirer, N. G.; Reuther, E.; Müllen, K. *Chem.—Eur. J.* **2005**, *11*, 3959. (f) Pschirer, N. G.; Kohl, C.; Nolde, F.; Qu, J.; Müllen, K. *Angew. Chem., Int. Ed.* **2006**, *45*, 1401. (g) Jung, C.; Müller, B. K.; Lamb, D. C.; Nolde, F.; Müllen, K.; Bräuchle, C. *J. Am. Chem. Soc.* **2006**, *128*, 5283.

(17) (a) For a recent review on multichromophoric PDI molecules, see: Langhals, H. *Helv. Chim. Acta* **2005**, *88*, 1309. Examples of multichromophoric PDI molecules are included in: (b) Langhals, H.; Gold, J. *J. Prakt. Chem.* **1996**, *338*, 654. (c) Langhals, H.; Ismael, R. *Eur. J. Org. Chem.* **1998**, 1915. (d) Langhals, H.; Speckbacker, M. *Eur. J. Org. Chem.* **2001**, 2481. (e) Wang, W.; Li, L.-S.; Helms, G.; Zhou, H. H.; Li, A. D. Q. *J. Am. Chem. Soc.* **2003**, *125*, 1120. (f) van der Boom, T.; Hayes, R. T.; Zhao, Y.; Bushard, P. J.; Weiss, E. A.; Wasielewski, M. R. *J. Am. Chem. Soc.* **2002**, *124*, 9582. (g) Rybtchinski, B.; Sinks, L. E.; Wasielewski, M. R. *J. Am. Chem. Soc.* **2004**, *126*, 12268. (h) Rybtchinski, B.; Sinks, L. E.; Wasielewski, M. R. *J. Phys. Chem. A* **2004**, *108*, 7497.

(18) Pisula, W.; Kastler, M.; Wasserfallen, D.; Robertson, J. W. F.; Nolde, F.; Kohl, C.; Müllen, K. *Angew. Chem., Int. Ed.* **2006**, *45*, 819.

(19) For recent reviews on functional supramolecular architectures based on PDI dyes, see: (a) Würthner, F. *Chem. Commun.* **2004**, 1564. (b) Eelemans, J. A. A. W.; van Hameren, R.; Nolte, R. J. M.; Rowan, A. E. *Adv. Mater.* **2006**, *18*, 1251.

(20) (a) Yoshida, N.; Ishizuka, T.; Yofu, K.; Murakami, M.; Miyasaka, H.; Okada, T.; Nagata, Y.; Itaya, A.; Cho, H. S.; Kim, D.; Osuka, A. *Chem.—Eur. J.* **2003**, *9*, 2854. (b) Tomizaki, K.-Y.; Thamyongkit, P.; Loewe, R. S.; Lindsey, J. S. *Tetrahedron* **2003**, *59*, 1191. (c) Kelley, R. F.; Tauber, M. J.; Wasielewski, M. R. *J. Am. Chem. Soc.* **2006**, *128*, 4779.

(21) (a) Guo, X.; Zhang, D.; Zhang, H.; Fan, Q.; Xu, W.; Ai, X.; Fan, L.; Zhu, D. *Tetrahedron* **2003**, *59*, 4843. (b) Leroy-Lhez, S.; Baffreau, J.; Perrin, L.; Levillain, E.; Allain, M.; Blesa, M.-J.; Hudhomme, P. *J. Org. Chem.* **2005**, *70*, 6313.

(22) You, C.-C.; Würthner, F. *J. Am. Chem. Soc.* **2003**, *125*, 9716.

(23) Tian, H.; Liu, P.-H.; Zhu, W.; Gao, E.; Wu, D.-J.; Cai, S. *J. Mater. Chem.* **2000**, *10*, 2708.

(24) Takahashi, M.; Morimoto, H.; Miyake, K.; Yamashita, M.; Kawai, H.; Sei, Y.; Yamaguchi, K. *Chem. Commun.* **2006**, 3084.

(25) Langhals, H.; Saulich, S. *Chem.—Eur. J.* **2002**, *8*, 5630.

(26) Wescott, L. D.; Mattern, D. L. *J. Org. Chem.* **2003**, *68*, 10058.

(27) Yilmaz, M. D.; Bozdemir, O. A.; Akkaya, E. U. *Org. Lett.* **2006**, *8*, 2871.

(28) (a) Hua, J.; Meng, F.; Ding, F.; Tian, H. *Chem. Lett.* **2004**, *33*, 432. (b) Gómez, R.; Segura, J. L.; Martín, N. *Org. Lett.* **2005**, *7*, 717.

(29) (a) Weil, T.; Wiesler, U. M.; Herrmann, A.; Bauer, R.; Hofkens, J.; De Schryver, F. C.; Müllen, K. *J. Am. Chem. Soc.* **2001**, *123*, 8101. (b) De Belder, G.; Schweitzer, G.; Jordens, S.; Lor, M.; Mitra, S.; Hofkens, J.; De Feyter, S.; van der Auweraer, M.; Herrmann, A.; Weil, T.; Müllen, K.; De Schryver, F. C. *ChemPhysChem* **2001**, *1*, 49. (c) Weil, T.; Reuther, E.; Müllen, K. *Angew. Chem., Int. Ed.* **2002**, *41*, 1900. (d) Gronheid, R.; Hofkens, J.; Köhn, F.; Weil, T.; Reuther, E.; Müllen, K.; De Schryver, F. C. *J. Am. Chem. Soc.* **2002**, *124*, 2418. (e) Cotlet, M.; Masuo, S.; Luo, G.; Hofkens, J.; van der Auweraer, M.; Verhoeven, J.; Müllen, K.; Xie, X. S.; De Schryver, F. C. *Proc. Natl. Acad. Sci. U.S.A.* **2004**, *101*, 14343. (f) De Schryver, F. C.; Vosch, T.; Cotlet, M.; van der Auweraer, M.; Müllen, K.; Hofkens, J. *Acc. Chem. Res.* **2005**, *38*, 514. (g) Cotlet, M.; Vosch, T.; Habuchi, S.; Weil, T.; Müllen, K.; Hofkens, J.; De Schryver, F. C. *J. Am. Chem. Soc.* **2005**, *127*, 9760.

(30) (a) You, C.-C.; Saha-Möller, C. R.; Würthner, F. *Chem. Commun.* **2004**, 2030. (b) Chen, S.; Liu, Y.; Qiu, W.; Sun, X.; Ma, Y.; Zhu, D. *Chem. Mater.* **2005**, *17*, 2208. (c) Cremer, J.; Mena-Osteritz, E.; Pschierer, N. G.; Müllen, K.; Bäuerle, P. *Org. Biomol. Chem.* **2005**, *3*, 985.

(31) Neuteboom, E. E.; Meskers, S. C. J.; van Hal, P. A.; van Duren, J. K. J.; Meijer, E. W.; Janssen, R. A. J.; Dupin, H.; Pourtois, G.; Cornil, J.; Lazzaroni, R.; Brédas, J.-L.; Beljonne, D. *J. Am. Chem. Soc.* **2003**, *125*, 8625.

(32) Miura, A.; Chen, Z.; Uji-i, H.; De Feyter, S.; Zdanowska, M.; Jonkheijm, P.; Schenning, A. P. H. J.; Meijer, E. W.; Würthner, F.; De Schryver, F. C. *J. Am. Chem. Soc.* **2003**, *125*, 14968.

(33) Neuteboom, E. E.; Beckers, E. H. A.; Meskers, S. C. J.; Meijer, E. W.; Janssen, R. A. J. *Org. Biomol. Chem.* **2003**, *1*, 198.

(34) Jonkheijm, P.; Sutzmann, N.; Chen, Z.; de Leeuw, D. M.; Meijer, E. W.; Schenning, A. P. H. J.; Würthner, F. *J. Am. Chem. Soc.* **2006**, *128*, 9535.

(35) Holman, M. W.; Liu, R.; Zang, L.; Yan, P.; DiBenedetto, S. A.; Bowers, R. D.; Adams, D. M. *J. Am. Chem. Soc.* **2004**, *126*, 16126.

(36) Ko, H. C.; Kim, S.-H.; Choi, W.; Moon, B.; Lee, H. *Chem. Commun.* **2006**, 69.

(37) (a) Baier, J.; Pösch, P.; Gmann, G.; Schmidt, H.-W.; Seilmeier, A. *J. Chem. Phys.* **2001**, *114*, 6739. (b) Lindner, S. M.; Thelakkat, M. *Macromolecules* **2004**, *37*, 8832.

(38) Hernando, J.; de Witte, P. A. J.; van Dijk, E. M. H. P.; Korterik, J.; Nolte, R. J. M.; Rowan, A. E.; García-Parajó, M. F.; van Hulst, N. F. *Angew. Chem., Int. Ed.* **2004**, *43*, 4045.

(39) (a) Dotcheva, D.; Klapper, M.; Müllen, K. *Macromol. Chem. Phys.* **1994**, *195*, 1995. (b) Liu, Y.; Yang, C.; Li, Y.; Wang, S.; Zhuang, J.; Liu, H.; Wang, N.; He, X.; Zhu, D. *Macromolecules* **2005**, *38*, 716.

(40) (a) Dobrawa, R.; Kurth, D. G.; Würthner, F. *Polym. Prepr.* **2004**, *45*, 378. (b) Dobrawa, R.; Lysetska, M.; Ballester, P.; Grüne, M.; Würthner, F. *Macromolecules* **2005**, *38*, 1315.

(41) Goldsmith, R. H.; Sinks, L. E.; Kelley, R. F.; Betzen, L. J.; Liu, W.; Weiss, E. A.; Ratner, M. A.; Wasielewski, M. R. *Proc. Natl. Acad. Sci. U.S.A.* **2005**, *102*, 3540.

(42) (a) Ego, C.; Marsitzky, D.; Becker, S.; Zhang, J.; Grimsdale, A. C.; Müllen, K.; MacKenzie, J. D.; Silva, C.; Friend, R. H. *J. Am. Chem. Soc.* **2003**, *125*, 437. (b) Becker, S.; Ego, C.; Grimsdale, A. G.; List, E. J. W.; Marsitzky, D.; Pogantsch, A.; Setayesh, S.; Leising, G.; Müllen, K. *Synth. Met.* **2002**, *125*, 73.

(43) Feng, L.; Chen, Z. *Polymer* **2005**, *46*, 3952.

(44) (a) Ford, W. E.; Kamat, P. V. *J. Phys. Chem.* **1987**, *91*, 6373. (b) Akimoto, S.; Ohmori, A.; Yamazaki, I. *J. Phys. Chem. B* **1997**, *101*, 3753 and references therein.

(45) (a) Würthner, F.; Thalacker, C.; Diele, S.; Tschierske, C. *Chem.—Eur. J.* **2001**, *7*, 2245. (b) Balakrishnan, K.; Datar, A.; Naddo, T.; Huang, J.; Oitker, R.; Yen, M.; Zhao, J.; Zang, L. *J. Am. Chem. Soc.* **2006**, *128*, 7390. (c) Sugiyasu, K.; Fujita, N.; Shinkai, S. *Angew. Chem., Int. Ed.* **2004**, *43*, 1229. (d) van Herrikhuyzen, J.; Syamakumari, A.; Schenning, A. P. H. J.; Meijer, E. W. *J. Am. Chem. Soc.* **2004**, *126*, 10021. (e) Schenning, A. P. H. J.; van Herrikhuyzen, J.; Jonkheijm, P.; Chen, Z.; Würthner, F.; Meijer, E. W. *J. Am. Chem. Soc.* **2002**, *124*, 10252. (f) Schenning, A. P. H. J.; Meijer, E. W. *Chem. Commun.* **2005**, 3245. (g) Hoeben, F. J. M.; Jonkheijm, P.; Meijer, E. W.; Schenning, A. P. H. J. *Chem. Rev.* **2005**, *105*, 1491. (h) Nguyen, T.-Q.; Martel, R.; Avouris, P.; Bushey, M. L.; Brus, L.; Nuckolls, C. *J. Am. Chem. Soc.* **2004**, *126*, 5234.

(46) (a) Giaimo, J. M.; Gusev, A. V.; Wasielewski, M. R. *J. Am. Chem. Soc.* **2002**, *124*, 8530. (b) Ahrens, M. J.; Sinks, L. E.; Rybtchinski, B.; Liu, W.; Jones, B. A.; Giaimo, J. M.; Gusev, A. V.; Goshe, A. J.; Tiede, D. M.; Wasielewski, M. R. *J. Am. Chem. Soc.* **2004**, *126*, 8284.

(47) Li, X.; Sinks, L. E.; Rybtchinski, B.; Wasielewski, M. R. *J. Am. Chem. Soc.* **2004**, *126*, 10810.

(48) Selected references on the Suzuki coupling: (a) Suzuki, A. *Chem. Commun.* **2005**, *38*, 4759. (b) Suzuki, A. *Proc. Jpn. Acad.* **2004**, *80*, 359. (c) Nicolau, K. C.; Bulger, P. G.; Sarlah, D. *Angew. Chem., Int. Ed.* **2005**, *44*, 4442. (d) Li, Ch.-J. *Chem. Rev.* **2005**, *105*, 3095. (e) Miyaura, N.; Yanagi, T.; Suzuki, A. *Synth. Commun.* **1981**, *11*, 513. (f) Wallow, T. I.; Novak, B. M. *J. Am. Chem. Soc.* **1991**, *113*, 7411. (g) Suzuki, A. *Acc. Chem. Res.* **1982**, *15*, 178.

(49) Marcos Ramos, A.; Rispens, M. T.; van Duren, J. K.; Hummelen, J. C.; Janssen, R. A. J. *J. Am. Chem. Soc.* **2001**, *123*, 6714.

(50) (a) Segura, J. L.; Gómez, R.; Reinold, E.; Bäuerle, P. *Org. Lett.* **2005**, *7*, 2345. (b) Segura, J. L.; Gómez, R.; Blanco, R.; Reinold, E.; Bäuerle, P. *Chem. Mater.* **2006**, *18*, 2834.

(51) Brunner, K.; de Kok-van Breemen, M. M.; Langeveld, B. M. W.; Kiggen, N. M. M.; Bastiaansen, J. J. A. M.; Hofstraat, J. W.; Boerner, H. F.; Schoo, H. F. M. PCT Int. Appl. 2004, WO 2004072205 A2 20040826.

(52) (a) Kowitz, C.; Wegner, G. *Tetrahedron* **1996**, *53*, 15553. (b) Goodson, F. E.; Novak, B. M. *Macromolecules* **1997**, *30*, 6047.

(53) Wang, Ch.; Batsanov, A. S.; Bryce, M. R.; Sage, I. *Org. Lett.* **2004**, *6*, 2181.

(54) Dudek, S. P.; Pouderoijen, M.; Abbel, R.; Schenning, A. H. P.; Meijer, E. W. *J. Am. Chem. Soc.* **2005**, *127*, 11763.

(55) Langhals, H. *Heterocycles* **1995**, *40*, 477.

(56) Demmig, S.; Langhals, H. *Chem. Ber.* **1988**, *121*, 225.

(57) Salbeck, J.; Kunkely, H.; Langhals, H.; Saalfrank, R. W.; Daub, J. *Chimia* **1989**, *43*, 6.

(58) In ref 57 the reduction potentials were measured in acetonitrile vs Fc/Fc^+; the different conditions can explain that the reported values

of −0.93 and −1.15 eV for phenyl-substituted and −0.98 and −1.22 eV for alkyl-substituted PDIs slightly differ from our values.

(59) Langhals, H.; Demmig, S.; Huber, H. *Spectrochim. Acta* **1998**, *44A*, 1189.

(60) (a) Ford, W. E. *J. Photochem.* **1987**, *37*, 189. (b) Wang, W.; Han, J. J.; Wang, L.-Q.; Li, L.-S.; Shaw, W. J.; Li, A. D. Q. *Nanolett.* **2003**, *3*, 455.

(61) (a) So, F. F.; Forrest, S. R. *Phys. Rev. Lett.* **1991**, *66*, 2649. (b) Hennessy, M. H.; Soos, Z. G.; Pascal, R. A.; Girlando, A. *Chem. Phys.* **1999**, *245*, 199. (c) Li, A. D. Q.; Wang, W.; Wang, L.-Q. *Chem.—Eur. J.* **2003**, *9*, 4594. (d) Würthner, F.; Thalacker, C.; Sautter, A.; Schartel, W.; Ibach, W.; Hollricher, O. *Chem.—Eur. J.* **2000**, *6*, 3871.

(62) Neuteboom, E. E.; Meskers, S. C. J.; Meijer, E. W.; Janssen, R. A. J. *J. Macromol. Chem. Phys.* **2004**, *205*, 217.

(63) The radius of the PDI anion was estimated from the density of *N*,*N*′-dimethylperylene-3,4:9,10-tetracarboxylic diimide determined from the X-ray crystallographic data (Hádicke, E.; Graser, F. *Acta Crystallogr. C* **1986**, *42*, 189). However, it is more difficult to estimate a radius for the PFP cation. We have estimated a radius of 5 Å, analogous to previous radii for conjugated systems of similar length (Peeters, E.; van Hal, P. A.; Knol, J.; Brabec, C. J.; Sariciftci, N. S.; Hummelen, J. C.; Janssen, R. A. J. *J. Phys. Chem. B* **2000**, *104*, 10174). If a much larger value of, e.g., 10 Å is taken instead, the calculated free energy of the charge separated state (E_{CS}) only decreases slightly from 2.16 to 1.93 eV in toluene and from 1.61 to 1.56 eV in chlorobenzene and remains unaltered (1.47 eV) for dichloromethane.

(64) Katoh, R.; Sinha, S.; Murata, S.; Tachiya, M. *J. Photochem. Photobiol. A* **2001**, *145*, 23.

(65) Weller, A. *Z. Phys. Chem. (Muenchen, Ger.)* **1982**, *133*, 93.

(66) (a) Khajehpour, M.; Kaufmann, J. F. *J. Phys. Chem. A* **2001**, *105*, 10316 and references therein. (b) Reynolds, L. J.; Gardecki, A.; Frankland, S. J. V.; Horng, M. L.; Maroncelli, M. *J. Phys. Chem.* **1996**, *100*, 10337. (c) Jeon, J.; Kim, H. J. *J. Solution Chem.* **2001**, *30*, 849.

(67) A value of $\epsilon_{eff} = 4.3$ was calculated for toluene using a solute with $r = 4.3$ Å by Dorairaj et al.: Dorairaj, S.; Kim, H. J. *J. Phys. Chem. A* **2002**, *106*, 2322.

(68) Beckers, E. H. A.; Meskers, S. C. J.; Schenning, A. P. H. J.; Chen, Z.; Würthner, F.; Janssen, R. A. J. *J. Phys. Chem. A* **2004**, *108*, 6933.

(69) Fonseca, S. M.; Pina, J.; Arnaut, L. G.; Seixas de Melo, J.; Burrows, H. D.; Chattopadhyay, N.; Alcácer, L.; Charas, A.; Morgado, J.; Monkman, A. P.; Assawapirom, U.; Scherf, U.; Edge, R.; Navaratnam, S. *J. Phys. Chem. B* **2006**, *110*, 8278.

(70) (a) Ford, W. E.; Hiratsuka, H.; Kamat, P. V. *J. Phys. Chem.* **1989**, *93*, 6692. (b) Salbeck, J. *J. Electroanal. Chem.* **1992**, *340*, 169. (c) Würthner, F.; Sautter, A. *Chem. Commun.* **2000**, 445.

(71) Wei, X.; Vardeny, Z. V.; Sariciftci, N. S.; Heeger, A. J. *Phys. Rev. B* **1996**, *53*, 2187.

(72) (a) Kim, Y. H.; Spiegel, D.; Hotta, S.; Heeger, A. J. *Phys. Rev. B* **1988**, *38*, 5490. (b) Janssen, R. A. J.; Christiaans, M. P. T.; Hare, C.; Martín, N.; Sariciftci, N. S.; Heeger, A. J.; Wudl, F. *J. Chem. Phys.* **1995**, *103*, 8840.

(73) Raul-Berthelot, J.; Cariou, M.; Tahri-Hassani, J. *J. Electroanal. Chem.* **1996**, *402*, 203.

(74) Langhals, H.; Karolin, J.; Johanssonet, B. A. *J. Chem. Soc., Faraday Trans.* **1998**, *94*, 2919.

MA070026B